Searching for R-Parity Violation at Run-II of the Tevatron

B. Allanach[1], H. Baer[2], S. Banerjee[3], E.L. Berger[4], M. Chertok[5], F. de Campos[6], K. Cheung[7], A. Dedes[8], M.A. Diaz[2], H. Dreiner[8], O.J.P. Eboli[9,10], J. Gunion[7], B.W. Harris[4], J. Hewett[11], M.B. Magro[10], N.K. Mondal[3], V.S. Narasimham[3], L. Navarro[12], N. Parua[3], W. Porod[12,13], D.A. Restrepo[12], P. Richardson[14], T. Rizzo[11], M.H. Seymour[8], Z. Sullivan[4], J.W.F. Valle[12]

Edited by: H. Dreiner[6]

[1] *DAMTP, University of Cambridge, Cambridge, CB3 9EW, UK*
[2] *Department of Physics, Florida State University, Tallahassee, FL 32306, USA*
[3] *Tata Inst. of Fundamental Research, Bombay, India*
[4] *Argonne National Laboratory, Argonne, IL 60439*
[5] *Texas A&M University, College Station, TX 77843,*
[6] *Depart. de Física y Química, Univ. Estadual Paulista, Guaratinguetá, Brasil*
[7] *Department of Physics, University of California, Davis, CA 95616, USA*
[8] *Rutherford Appleton Laboratory, Chilton, Didcot OX11 0QX, U.K.*
[9] *Instituto de Física Teórica, Univ. Estadual Paulista, Sao Paulo, Brasil*
[10] *University of Wisconsin, Madison, WI 53706, USA*
[11] *Stanford Linear Accelerator, Stanford, CA 94309*
[12] *Departamento de Física Teórica, IFIC-CSIC, Univ. de Valencia, Spain*
[13] *Insitut für Theoretische Physik, Universität Wien, Austria*
[14] *Depart. of Theoret. Physics, University of Oxford, Oxford OX1 3NP, U.K.*

Abstract. We present an outlook for possible discovery of supersymmetry with broken R-parity at Run II of the Tevatron. We first present a review of the literature and an update of the experimental bounds. In turn we then discuss the following processes:
1. Resonant slepton production followed by $\not{R}_p$ decay, (a) via LQD^c and (b) via LLE^c.
2. How to distinguish resonant slepton production from Z' or W' production.
3. Resonant slepton production followed by the decay to neutralino LSP, which decays via LQD^c.
4. Resonant stop production followed by the decay to a chargino, which cascades to the neutralino LSP.
5. Gluino pair production followed by the cascade decay to charm squarks which decay directly via $L_1Q_2D_1^c$.
6. Squark pair production followed by the cascade decay to the neutralino LSP which decays via $L_1Q_2D_1^c$.
7. MSSM pair production followed by the cascade decay to the LSP which decays (a) via LLE^c, (b) via LQD^c, and (c) via $U^cD^cD^c$, respectively.
8. Top quark and top squark decays in spontaneous $\not{R}_p$.

I INTRODUCTION

H. Dreiner

The chiral superfields of the supersymmetric Standard Model are

$$L_i\ (1,2,-\frac{1}{2}),\quad E_i^c\ (1,1,1),\quad H_1\ (1,2,-\frac{1}{2}),\quad H_2\ (1,2,\frac{1}{2}),$$
$$Q_i\ (3,2,\frac{1}{6}),\quad U_i^c\ (3,1,-\frac{2}{3}),\quad D_i^c\ (3,1,\frac{1}{3}). \tag{1}$$

In parentheses we have given the quantum numbers under the Standard Model gauge group, $G_{SM} = SU(3) \times SU(2) \times U(1)$. $i = 1, 2, 3$ is a generation index. The most general superpotential for this field content is[1]

$$W = W_{MSSM} + W_{\not R_p}, \tag{2}$$

$$W_{\not R_p} = \frac{1}{2}\lambda_{ijk}\epsilon_{ab}L_i^a L_j^b E_k^c + \lambda'_{ijk}\epsilon_{ab}L_i^a Q_j^b D_k^c + \lambda''_{ijk}\epsilon_{xyz}U_i^{cx} D_j^{cy} D_k^{cz} + \kappa_i \epsilon_{ab} L_i^a H_2^b. \tag{3}$$

Here, W_{MSSM} is the superpotential of the MSSM containing the terms which give mass to the SM fermions. We do not further discuss it here. $i, j, k = 1, 2, 3$ are generation indices, $a, b = 1, 2$ are $SU(2)$ isospin indices, and $x, y, z = 1, 2, 3$ are $SU(3)$ colour indices. $\lambda, \lambda', \lambda''$ are dimensionless Yukawa couplings. κ_i are mass terms mixing the leptonic and Higgs doublets. The terms in $W_{\not R_p}$ violate the discrete and multiplicative symmetetry R-parity

$$R_p = (-1)^{3B+L+2S}, \tag{4}$$

where B is baryon-, L is lepton-number and S denotes the spin. It is the purpose of this chapter to investigate the phenomenological consequences of the superpotential terms $W_{\not R_p}$ at the Tevatron. For a recent review on R_p violation ($\not R_p$) see [1]. A very nice detailed overview of $\not R_p$ collider phenomenology is given in [2].

At the level of the superpotential, the terms $L_i H_2$ can be rotated away by a field redefinition [3]. When including the soft-breaking terms this is no longer true in general. However, we shall split our investigations into explicit R_p violation, where we neglect all contributions from the $L_i H_2$ mixing, and spontaneous $\not R_p$.

II EXPLICIT R-PARITY VIOLATION

A Existing Bounds

B. Allanach, A. Dedes, H. Dreiner

In Table 1, we show a recent compilation of indirect bounds on the $\not R_p$ Yukawa couplings [4,5,1,6]. We present the bounds at the 2σ level and give two significant figures where possible. The bounds depend on the mass of super partner and we give the functional dependence. For more detail on how the bounds are obtained see [4,5]. We ignore strict bounds from cosmology [7] because they are model dependent [8]. A discussion of the bounds on λ''_{ijk} is given in Sect. VIII.

B Outline of Signals and Summary of the Literature

The two main differences between the standard MSSM phenomenology and the phenomenology of explicit $\not R_p$ are

1. Single production of supersymmetric particles is possible. For example at a hadron collider we can have resonant slepton (charged and neutral) production via the operators $L_i Q_j \bar{D}_k$ and resonant squark production via the operators $\bar{U}_i \bar{D}_j \bar{D}_k$. The lowest order Feynman diagrams are shown in Figs. 1a. This lowers the kinematic threshold for the discovery of supersymmetry.

2. The lightest supersymmetric particle (LSP) is not stable, and can possibly decay in the detector. If the LSP is the lightest neutralino it can decay, for example, via the operator $L_i Q_j \bar{D}_k$, as shown in Fig. 2. However, since the LSP is not stable, the cosmological argument requiring it to be electrically and colour neutral no longer applies [20]. To date there have been no systematic studies of non-neutralino LSPs in the context of $\not R_p$. If the LSP is charged and has an appreciable lifetime (or is stable), it can be detected in a search for charged massive particles (CHAMPs).

A first systematic study of R-parity violating signals at hadron collider was presented in [21,22]. There are in principle two kinds of signals given by the two kinds of supersymmetric production.

---

[1] Note that ^{c} here refers to charge conjugation and is not a $SU(2)$ index.

TABLE 1. Latest 2σ limits on the magnitudes of weak scale trilinear R-parity violating couplings from indirect decays and perturbativity. We have made use of the data in [17]. The dependence on the relevant superparticle mass is shown explicitly. When the perturbativity bounds are more stringent than the empirical bounds for masses $m_{\tilde{l},\tilde{q}}$=1 TeV, then we display them in parentheses. Where a bound without parentheses has no explicit mass dependence shown, the mass dependence was too complicated to detail here and a degenerate sparticle spectrum of 100 GeV is assumed.

ijk	$\lambda_{ijk}(M_Z)$[a]	$\lambda'_{ijk}(M_Z)$[b]	$\lambda''_{ijk}(M_Z)$[c]
111	-	$5.2\times10^{-4}\times\dot{.}^{\rm m}$	-
112	-	$0.021\times\frac{m_{\tilde{s}_R}}{100\ \rm GeV}$	$10^{-15}\times(\frac{m_{\tilde{q}}}{\Lambda\ \rm GeV})^{5/2}$
113	-	$0.021\times\frac{m_{\tilde{b}_R}}{100\ \rm GeV}$	10^{-4}
121	$0.049\times\frac{m_{\tilde{e}_R}}{100\ \rm GeV}$	$0.043\times\frac{m_{\tilde{d}_R}}{100\ \rm GeV}$	$10^{-15}\times(\frac{m_{\tilde{q}}}{\Lambda\ \rm GeV})^{5/2}$
122	$0.049\times\frac{m_{\tilde{\mu}_R}}{100\ \rm GeV}$	$0.043\times\frac{m_{\tilde{s}_R}}{100\ \rm GeV}$	-
123	$0.049\times\frac{m_{\tilde{\tau}_R}}{100\ \rm GeV}$	$0.043\times\frac{m_{\tilde{b}_R}}{100\ \rm GeV}$	(1.23)
131	$0.062\times\frac{m_{\tilde{e}_R}}{100\ \rm GeV}$	$0.019\times\frac{m_{\tilde{t}_L}}{100\ \rm GeV}$	10^{-4}
132	$0.062\times\frac{m_{\tilde{\mu}_R}}{100\ \rm GeV}$	$0.28\times\frac{m_{\tilde{t}_L}}{100\ \rm GeV}$ (1.04)	(1.23)
133	$0.0060\sqrt{m_{\tilde{\tau}}/100\ \rm GeV}$	$1.4\times10^{-3}\sqrt{m_{\tilde{b}}/100\ \rm GeV}$	-
211	$0.049\times\frac{m_{\tilde{e}_R}}{100\ \rm GeV}$	$0.059\times\frac{m_{\tilde{d}_R}}{100\ \rm GeV}$	-
212	$0.049\times\frac{m_{\tilde{\mu}_R}}{100\ \rm GeV}$	$0.059\times\frac{m_{\tilde{s}_R}}{100\ \rm GeV}$	(1.23)
213	$0.049\times\frac{m_{\tilde{\tau}_R}}{100\ \rm GeV}$	$0.059\times\frac{m_{\tilde{b}_R}}{100\ \rm GeV}$	(1.23)
221	-	$0.18\times\frac{m_{\tilde{s}_R}}{100\ \rm GeV}$ (1.12)	(1.23)
222	-	$0.21\times\frac{m_{\tilde{s}_R}}{100\ \rm GeV}$ (1.12)	-
223	-	$0.21\times\frac{m_{\tilde{b}_R}}{100\ \rm GeV}$ (1.12)	(1.23)
231	$0.070\times\frac{m_{\tilde{e}_R}}{100\ \rm GeV}$	$0.18\times\frac{m_{\tilde{b}_L}}{100\ \rm GeV}$ (1.12)	(1.23)
232	$0.070\times\frac{m_{\tilde{\mu}_R}}{100\ \rm GeV}$	0.56 (1.04)	(1.23)
233	$0.070\times\frac{m_{\tilde{\tau}_R}}{100\ \rm GeV}$	$0.15\sqrt{m_{\tilde{b}}/100\ \rm GeV}$	-
311	$0.062\times\frac{m_{\tilde{e}_R}}{100\ \rm GeV}$	$0.11\times\frac{m_{\tilde{d}_R}}{100\ \rm GeV}$ (1.12)	-
312	$0.062\times\frac{m_{\tilde{\mu}_R}}{100\ \rm GeV}$	$0.11\times\frac{m_{\tilde{s}_R}}{100\ \rm GeV}$ (1.12)	0.50 (1.00)
313	$0.0060\sqrt{m_{\tilde{\tau}}/100\ \rm GeV}$	$0.11\times\frac{m_{\tilde{b}_R}}{100\ \rm GeV}$ (1.12)	0.50 (1.00)
321	$0.070\times\frac{m_{\tilde{e}_R}}{100\ \rm GeV}$	$0.52\times\frac{m_{\tilde{d}_R}}{100\ \rm GeV}$ (1.12)	0.50 (1.00)
322	$0.070\times\frac{m_{\tilde{\mu}_R}}{100\ \rm GeV}$	$0.52\times\frac{m_{\tilde{s}_R}}{100\ \rm GeV}$ (1.12)	-
323	$0.070\times\frac{m_{\tilde{\tau}_R}}{100\ \rm GeV}$	$0.52\times\frac{m_{\tilde{b}_R}}{100\ \rm GeV}$ (1.12)	0.50 (1.00)
331	-	0.45 (1.04)	0.50 (1.00)
332	-	0.45 (1.04)	0.50 (1.00)
333	-	0.45 (1.04)	-

[a] Updated bounds from Ref. [5,1]. Bounds on λ_{121}, λ_{122}, λ_{123} have been obtained from charged current universality [9]. Bounds on λ_{131}, λ_{132}, λ_{231}, λ_{232} and λ_{233} have been derived from [9] measurements of $R_\tau = \Gamma(\tau\to e\nu\bar{\nu})/\Gamma(\tau\to\mu\nu\bar{\nu})$ and $R_{\tau\mu} = \Gamma(\tau\to\mu\nu\bar{\nu})/\Gamma(\mu\to e\nu\bar{\nu})$ [17]. The bound on λ_{133} [10] has been obtained from the experimental limit on the electron neutrino mass [17].

[b] Bounds on λ'_{112}, λ'_{113}, λ'_{121}, λ'_{122}, and λ'_{123} have been obtained from charged current universality [9]. The bound on λ'_{111} has been derived from neutrinoless double beta decay [11,12] where $\dot{.}^{\rm m} = (m_{\tilde{e}}/100\ \rm GeV)^2\times(m_{\tilde{\chi}^0}/100\ \rm GeV)^{1/2}$, and on λ'_{131} from atomic parity violation [9,15]. This latter bound is at the 3σ level, since the data disagree with the standard model at the 2.5σ level [15]. The bound on λ'_{132} comes from the forward-backward asymmetry in e^+e^- collisions [9]. Bounds on λ'_{133}, λ'_{233} have been obtained from bounds on the neutrino masses [10] and on λ'_{211}, λ'_{212}, λ'_{213} from $R_\pi = \Gamma(\pi\to e\nu)/\Gamma(\pi\to\mu\nu)$ [9,5]. Bounds on λ'_{221}, λ'_{231} come from ν_μ deep inelastic scattering [9,5] and on λ'_{222}, λ'_{223} from the D-meson decays [5], $D\to Kl\nu$. The bounds without parentheses on λ'_{232}, λ'_{331}, λ'_{332}, λ'_{333} have been derived from $R_l = \Gamma(Z\to$ had$)/\Gamma(Z\to l\bar{l})$ for $m_{\tilde{q}} = 100$ GeV [13] and on λ'_{311}, λ'_{312}, λ'_{313} from $R_{\tau\pi} = \Gamma(\tau\to\pi\nu_\tau)/\Gamma(\pi\to\mu\nu_\mu)$ [9,5]. The bounds on the couplings λ'_{321}, λ'_{322} and λ'_{323} have been derived from D_s decays [5], *i.e.,* $R_{D_s} = \Gamma(D_s\to\tau\nu_\tau)/\Gamma(D_s\to\mu\nu_\mu)$. There are also bounds on λ'_{3j3} from R_b [16] but these are weak at 2σ level and thus not displayed.

[c] The indirect bounds on λ''_{ijk} existing in the literature are on λ''_{112} from double nucleon decay [14] ($\tilde{\Lambda}$ is a hadronic scale and it can be varied from 0.003 to 1 GeV and $(\frac{m_{\tilde{q}}}{\Lambda\ \rm GeV})^{5/2}$ from 2×10^{11} to 10^5 for $m_{\tilde{q}} = 100$ GeV) and on λ''_{113} from neutron oscillations [18,14] for $m_{\tilde{q}}$=100 GeV. For $m_{\tilde{q}}$=200 (600) GeV the bound on λ''_{113} is 0.002 (0.1). Bounds on λ''_{3jk} have been derived from $R_l = \Gamma(Z\to$ had$)/\Gamma(Z\to l\bar{l})$ at 1σ for $\tilde{m} = 100$ GeV [19] and, for heavy squark masses, is not more stringent than the perturbativity bound, which is

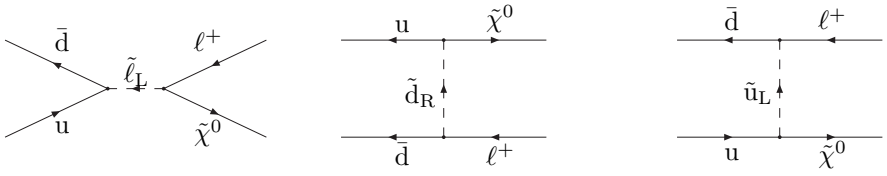

FIGURE 1. Production of $\tilde{\chi}^0 \ell^+$.

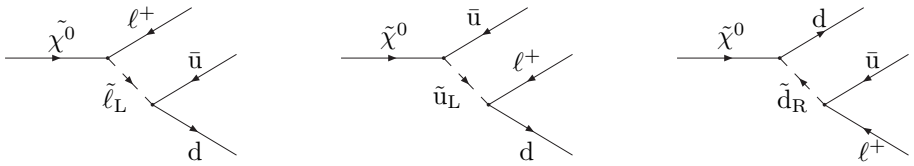

FIGURE 2. LQD decay of $\tilde{\chi}^0$. The neutralino is a Majorana fermion and decays to the charge conjugate final state as well.

1. Single Sparticle Production, *e.g.* $u + \bar{d} \to \ell^+$.
2. Pair production of Sparticles via MSSM couplings, *e.g.* $u + \bar{u} \to \tilde{q} + \tilde{\bar{q}}$.

In both cases the production is followed either by direct R-parity violating decays of the supersymmetric particles or by cascade decays to the LSP, which in turn decays via $\not{R}_p$. This latter decay can be prompt or delayed. If it is delayed it can lead to a detached vertex or decay outside the detector. To date only prompt decays have been considered. Within this report we also discuss delayed decays (see VIII and [23]) leading to detached vertices. The LSP decays outside the detector for small R-parity violating couplings, $\lambda, \lambda', \lambda'' \lesssim 10^{-5}$, [22,24]. The resonant production is then also suppressed and we thus retrieve the MSSM phenomenology, where sparticles are pair-produced and the LSP escapes detection. This is discussed in the contribution by the SUGRA working group.

In the following we summarize the possible signatures and indicate what work has already been performed. There is at present only one published experimental search for $\not{R}_p$ at hadron colliders [25]. A summary as well as the projection of this analysis for Run II is presented in Sect. VI. There is a preliminary D0 analysis publically available [26]. We present the extension of this analysis to Run II in Sect.VII. There *are* published results on searches for pair production of leptoquarks, which can be interpreted as searches for $\not{R}_p$ (see Sect.II B 2). In the following, most references are thus to theoretical work on specific signals.

1 Single Sparticle Production

At a hadron collider sneutrinos and charged leptons can be produced on resonance via the operator $L_i Q_j D^c_k$. They can then decay again via the same operator, another LQD^c operator, the operator $L_i L_j E^c$ or via the MSSM gaugino interactions. Thus we obtain the possible reactions

$$\bar{d}_j d_k \to \tilde{\nu}_i \to \left\{ \begin{array}{lll} \ell^+_m \ell'^-_n, & L_i L_m \bar{E}_n, & (a) \\ d_k \bar{d}_j, & L_i Q_j \bar{D}_k, & (b) \\ \nu_i \chi^0_m, & \text{MSSM}, & (c) \\ \ell^+_i \chi^-_m, & \text{MSSM}, & (d) \end{array} \right. , \quad u_j \bar{d}_k \to \tilde{\ell}^+_i \to \left\{ \begin{array}{lll} \ell^+_k \nu_j, & L_i L_j \bar{E}_k, & (e) \\ u_j \bar{d}_k, & L_i Q_j \bar{D}_k, & (f) \\ \ell^+_i \chi^0_m, & \text{MSSM}, & (g) \\ \nu_i \chi^+_m, & \text{MSSM}. & (h) \end{array} \right. \tag{5}$$

Here we have indicated the decay products of the slepton, as well as the coupling which leads to this decay. The decays to gauginos proceed via MSSM gauge couplings. Resonant slepton production was first considered in [21], where the production cross sections for the Tevatron were determined and the decays (5)a,b,e,f were compared to the background. The specific case of scalar tau production in (5)e was considered in [27] and compared to more recent Tevatron data on Drell-Yan di-lepton production. In Sect. III we investigate the

reactions (5)a,b,e,f in detail and compare them to exisiting Tevatron data. Furthermore the reactions (5)a,e can look identical in their final state to new gauge boson, W', Z', production and we also investigate how this can be disentangled in Sect. III. For both cases we use present data to project the search reach for Run II. In Sect. IV, we study for the first time the case of like-sign di-lepton production via the reactions (5)g. The focus is on a single dominant $\not{R}_p$ operator, so that the neutralino decays as $\chi^0 \to \ell^\pm + 2\,\text{jets}$, as shown in Fig.2. The analysis for the reaction (5)d is completely analogous.

The reactions for resonant squark production via the operators $U^c D^c D^c$ are

$$qq' \to \tilde{q}'' \to \begin{cases} (\ell,\nu)_i\, q, & L_i Q D^c, \quad (a) \\ qq', & U^c D^c D^c, \quad (b) \\ q\,(\chi^0_m, \tilde{g}), & \text{MSSM}, \quad (c) \\ q\,\chi^+_m, & \text{MSSM}. \quad (d) \end{cases} \tag{6}$$

The two-jet production via (6)b was considered in [21]. In special cases the reactions (5)f and (6)b can lead to single top quark production. This has been studied in [28]. In Sect.V we study the reaction (6)d in detail, where the produced squark is a stop. On resonance, the reaction (6)c is kinematically blocked because of the final state top quark. The chargino of reaction (6)d cascade decays to the lightest neutralino in a semi-leptonic decay and the charged lepton is used for detection. The dominant decay of the neutrlino is also suppressed because of the top quark in the final state and thus decays outside the detector.

2 Sparticle Pair Production

For $\not{R}_p$ couplings $\lambda, \lambda', \lambda'' \lesssim 10^{-3}$ resonance production is no longer viable. We then expect pair production of supersymmetric particles to dominate. The main reactions are

$$p\bar{p} \to \{\tilde{g}\tilde{g},\ \tilde{g}\tilde{q},\ \tilde{q}\tilde{q},\ \tilde{\chi}^0_i\tilde{\chi}^0_j,\ \tilde{\chi}^+_i\tilde{\chi}^-_j,\ \tilde{\chi}^0_i\tilde{\chi}^+_j,\ \tilde{\ell}^+\tilde{\ell}^-,\ \tilde{\nu}\tilde{\nu},\ \tilde{\ell}^+\tilde{\nu}\} \tag{7}$$

The supersymmetric particles can undergo cascade decays to the LSP as in the MSSM. The LSP, which we here assume to be the lightest neutralino then decays via $\not{R}_p$

$$\tilde{\chi}^0_1 \to \begin{cases} \ell^\pm_i \ell^\mp_k \nu_j, & L_i L_j E^c_k, \quad (a) \\ \ell^\pm_i + 2\,\text{jets}, & L_i Q_j D^c_k, \quad (b) \\ \nu + 2\,\text{jets}, & L_i Q_j D^c_k, \quad (c) \\ 3\,\text{jets}, & U^c_i D^c_j D^c_k. \quad (d) \end{cases} \tag{8}$$

The resulting reactions were first considered in [21] and classified in [22]. Gluino and squark pair production were first analysed in detail and compared to CDF data in [29]. In each case, the MSSM cascade decays were explicitly neglected, giving branching ratio 1 for the decay to the neutralino LSP. In [30] the production of the electroweak gauginos was studied focusing on the reactions

$$p\bar{p} \to \begin{cases} \chi^\pm_1\chi^0_2 & \to & \begin{cases} (\chi^0_1\ell^\pm\nu)(\chi^0_1\ell'^+\ell'^-), & (a) \\ (\chi^0_1\ell^+\nu)(\chi^0_1\ell'^-\nu), & (b) \end{cases} \\ \chi^\pm_1\chi^0_1 & \to & (\chi^0_1\ell^\pm\nu)\,\chi^0_1, \quad (c) \\ \chi^+_1\chi^-_1 & \to & (\chi^0_1\ell^+\nu)(\chi^0_1\ell'^-\nu), \quad (d) \end{cases} \tag{9}$$

followed by the decay of the LSP via the operator $L_i L_j E^c_k$ as in (8). In this case the discovery reach is significantly above that of the MSSM.

In Ref. [31] *all* the production mechanisms given in Eq.(7) were studied simultaneously in the framework of minimal SUGRA to see what combined contribution there would be to several possible discovery signals: (i) quartic-leptons, (ii) tri-leptons, (iii) opposite sign di-leptons, (iv) same-sign di-leptons, and (v) missing transverse energy. Each signature was compared for the two scenarios of an LSP decaying via LLE^c and $U^c D^c D^c$, respectively. In Sect.VI we study the case of pair production followed by cascade decay to the LSP including a detector simulation. The LSP decays via the operator LLE^c. The results are compared to the present Tevatron data and projected to a discovery reach for Run II. In Sect.VII we investigate in detail the potential at Run II for the di-lepton signature in the case of a dominant LQD^c operator. In [32] the previous analysis of gluino and squark pair production of [29] was extended to include cascade decays and investigate the

search reach in the gluino and squark mass at the Tevatron. In Sect. VIII, we investigate the possibility of the LSP decaying via $U^cD^cD^c$ to three jets, where the chargino and neutralino mass are nearly degenerate, thus making the cascade leptons of [31] too soft for detection. This is the worst case scenario for supersymmetry searches.

In February, 1997 both HERA experiments announced an anomaly in their high Q^2 deep inelastic scattering data [33]. This has not been confirmed in the later data but it has also not been excluded yet. The initial anomaly could naturally be explained in terms of resonant production of squarks via $\not{R}_p$ [34] or as resonant production of leptoquarks [35]. It lead to an increased interest in the searches for squarks and leptoquarks at the Tevatron. In leptoquark pair production at the Tevatron, the leptoquarks directly decay to a lepton and a quark. The experimental signature is equivalent to pair produced squarks decaying directly via the LQD^c operators. This is thus a distinct signature from the cascade decay to the LSP. We can interpret the leptoquark searches [36,37] in terms of $\not{R}_p$ with large λ'_{ijk} Yukawa couplings. We would expect additional decays for the squarks to gauginos. So the leptoquark mass bound corresponds to an excluded region in the mass branching ratio, $BR(\tilde{q} \to \ell + q')$, plane. The present Tevatron data [36–38] excludes the solution of the HERA anomaly where $BR(\tilde{q} \to \ell + q') = 1$ and severely constrains the case where $BR(\tilde{q} \to \ell + q') < 1$ [39]. In Sect. VI we present a study of gluino pair production followed by the cascade decay to charm squarks (as motivated by the HERA anomaly) which in turn decay directly via $L_1Q_2D_1^c$, *i.e.* not via the LSP. We also investigate the pair production of squarks followed by the cascade decay to the LSP which decays via $L_1Q_2D_1^c$. This focuses particularly on the $\not{R}_p$ interpretation of the HERA data which is not covered by the leptoquark searches.

PART 1: Resonant SParticle Production

III R-PARITY VIOLATING DECAY OF THE SLEPTON AND IDENTIFICATION

J. Hewett, T. Rizzo[2]

In this section, we concentrate on the two sets of trilinear L-violating terms in $W_{\not{R}_p}$, and the case of single charged or neutral slepton production via $q\bar{q}^{(')}$ annihilation at the Tevatron through the λ' couplings. If this slepton decays to opposite sign leptons (through the λ couplings) then an event excess, clustered in mass, will be observed in the Drell-Yan channel similar to that expected for a new neutral or charged gauge boson, Z' or W'. In addition, both $\tilde{\ell}$ and $\tilde{\nu}$ resonances may decay hadronically via the same vertices that produced them, leading to potentially observable peaks in the dijet invariant mass distribution. Thus resonant slepton production, first discussed in Ref. [21,40], offers a unique way to explore the $\not{R}_p$ model parameter space at hadron colliders. It is important that $\not{R}_p$ also allows for other SUSY particles, such as $\tilde{t}$ and/or $\tilde{b}$, to be exchanged in the non-resonant $t, u-$channels and also contribute to Drell-Yan events. However, it can be easily shown that their influence on cross sections and various distributions will be quite small if the low energy constraints on the Yukawa couplings are satisfied. [35] The questions addressed in this analysis are: (i) what are the mass and coupling reaches for slepton resonance searches at the Tevatron in the Drell-Yan and dijet channels and (ii) how can slepton resonances, once discovered, be distinguished from Z', W' production.

3 Drell-Yan Channel for Sleptons

From the bounds in Section II A, we see that the coupling responsible for first generation slepton production, λ'_{111}, is much too restricted to generate a sizable cross section. However the bounds on the couplings for second and third generation slepton production and decay are all of similar numerical values and allow for a reasonably sized signal. In addition, the background free $e^{\pm}\mu^{\mp}$ signature is also possible.

In the case of Drell-Yan production the search reach analysis is straightforward being nearly identical to that used for new gauge boson production, apart from acceptance issues due to the differences between spin-0 and spin-1 resonances. Since sleptons are expected to be narrow, the narrow width approximation is adequate and the analysis presented in Ref. [41] can be directly followed. In addition to the slepton mass the only other

[2] Work supported by the Department of Energy, Contract DE-AC03-76SF00515

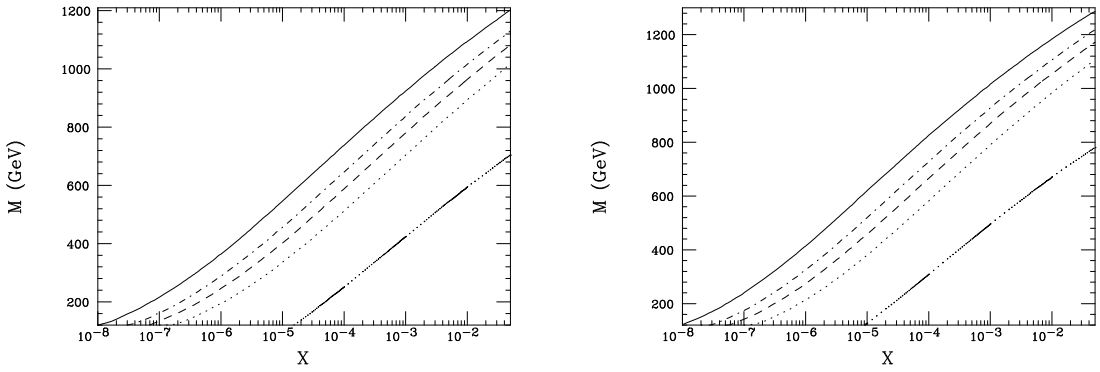

FIGURE 3. Discovery regions (lying below the curves) in the mass-coupling plane for $\not{R}_p$ resonances in the neutral (left) and charged (right) Drell-Yan channels at the Run II Tevatron. From top to bottom the curves correspond to integrated luminosities of 30, 10, 5 and 2 fb^{-1}. The estimated reach for Run I is given by the lowest curve. The parameter X is defined in the text.

parameter in the calculation is the product of the appropriate Yukawa couplings, λ', from the initial state $d\bar{u}$ or $d\bar{d}$ coupling vertex, and the slepton's leptonic branching fraction, B_ℓ. Denoting this product as $X = (\lambda')^2 B_\ell$, we obtain the 95% C.L. search reach as a function of X in both the charged and neutral channels. These results are displayed in Fig. 3 for various values of the integrated luminosity. Not only is it important to notice the very large mass reach of these colliders for sizeable values of $X \sim 10^{-3}$, but we should also observe the small X reach, $X \sim 10^{-(5-7)}$ and below, for relatively small slepton masses. These results show the rather wide opportunity available to discover slepton resonances over extended ranges of masses and couplings at the Tevatron. Note that for fixed values of X the search reach is greater in the charged current channel due to the higher parton luminosities in that case.

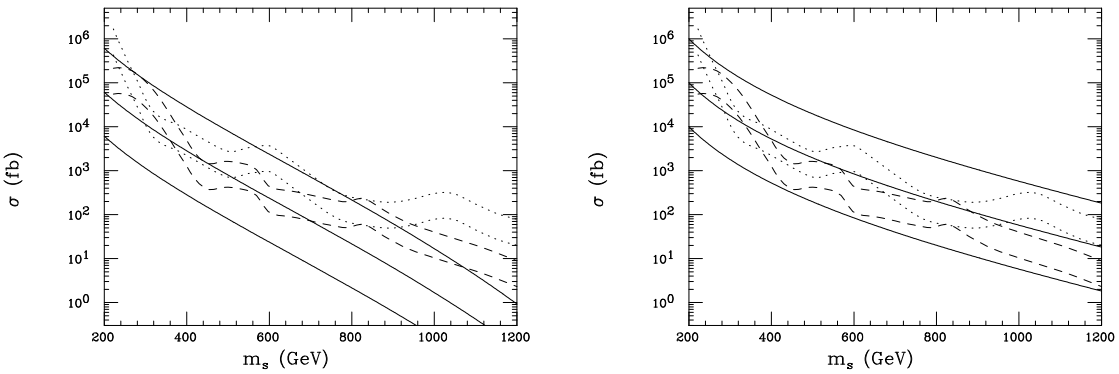

FIGURE 4. Cross sections for narrow dijet resonances (solid) at the 2 TeV Tevatron arising from $\tilde{\nu}$ (left) or $\tilde{\ell}$ (right) production in comparison to the anticipated search reaches of CDF (dots) and D0 (dashes). The upper(lower) curve for each experiment assumes an integrated luminosity of 2(30) fb^{-1}. The three solid curves from top to bottom correspond to slepton resonance predictions for Y=0.1, 0.01 and 0.001, respectively, where Y is defined in the text.

4 Di-Jet Decays of the Slepton

Since $d\bar{d}$ and/or $u\bar{d}$ annihilation are responsible for single slepton production, slepton resonance can also decay into these same fermion pairs. Hence $\tilde{\ell}$ or $\tilde{\nu}$ will have dijet decays which may appear as observable peaks above the conventional QCD backgrounds. Searches for such narrow dijet resonances have already been performed [42] at the Tevatron by both CDF and D0 during Run I. Using their results and scaling by

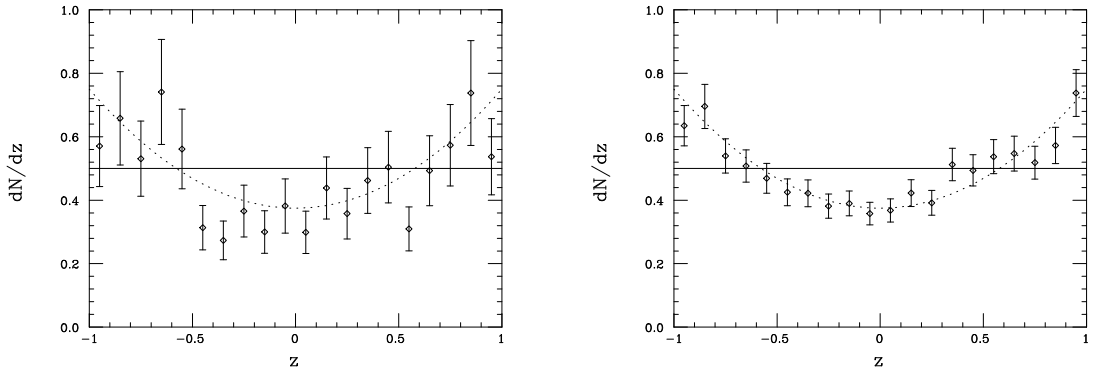

FIGURE 5. Comparison of the Monte Carlo generated normalized angular distribution for the leptons in Z' decay (data points) with that for a $\tilde{\nu}$ (solid curve) assuming a (left)400 event sample or a (right)2000 event sample; the displayed errors are purely statistical. The Z' is assumed to have no forward-backward asymmetry due to its fermionic couplings. A $1+z^2$ angular distribution is represented by the dotted curve.

appropriate factors of beam energy and integrated luminosities we may estimate the probable search reaches for CDF and D0 from Run II. Our estimates conform to the expectations given in Ref. [43]. The cross sections themselves are calculable in the narrow width approximation in terms of the product $Y = (\lambda')^2 B_{2j}$, where λ' is the Yukawa coupling and B_{2j} is the dijet branching fraction. The results are presented in Fig. 4. Here we see that for values of $Y \gtrsim 0.001 - 0.01$ the Tevatron will have a substantial mass reach for slepton induced dijet mass bumps during Run II. Note that as in the case of Drell-Yan production, larger cross sections for fixed Y occur in the charge current channel than in the neutral current case due to the larger parton luminosities. Unfortunately, if such a bump is observed it will not be straightforward to identify it as a slepton resonance.

5 *Distinguishing Sleptons from W', Z'*

Our next issue concerns the ability to determine that an observed resonance (or Jacobian peak) in the Drell-Yan channel is due to slepton production, instead of a new gauge boson, Z', W'. One clear signature for $\tilde{\nu}$ production would be the observation of $e\mu$ final states. These are not expected to occur in Z' models and would point to $\not{R}_p$. In addition, if the R_p conserving decay modes of the slepton dominate there will be no identification problem. If the $\not{R}_p$ modes dominate one should first look for universality violations, *e.g.*, if the resonance decays to only one of e^+e^- or $\mu^+\mu^-$ or if these two rates are substantially different. Most models with new gauge bosons do not have substantially different couplings to the first two fermion generations.

In the neutral current channel, *i.e.* , $\tilde{\nu}$ or Z' production, the forward-backward asymmetry A_{FB} in the leptonic decay distributions provides a good diagnostic tool. It is well-known that most models of Z' bosons have parity violating fermionic couplings which would lead to $A_{FB} \neq 0$. However, $\tilde{\nu}$, being spin-0, would always produce a null asymmetry. A_{FB} is more easily measured and requires less statistical power than does the reconstruction of the complete angular distribution. This is important since, whereas only 10 or so background free events would constitute a discovery, many more events, $\sim 100 - 200$ are required to determine the asymmetry. This implies that the reach for performing this test is somewhat, if not substantially, less than the discovery reach. For example, the Tevatron may discover a $\tilde{\nu}$ with a mass of 700 GeV for a certain value of X but only for masses below 500 GeV would there be enough statistics to extract A_{FB} for this same X value.

A more complex and interesting situation arises when the Z' naturally has $A_{FB} = 0$ as in, *e.g.* , some E_6 models [44]; in this case the on-resonance asymmetry data alone is insufficient. If A_{FB} could be measured throughout the resonance region, it would be possible to deduce through detailed line-shape studies whether or not the new contribution interferes with the SM amplitude (something that does not occur in the case of spin-0 $\tilde{\nu}$ production). However, finite dilepton mass resolution, especially for the $\mu^+\mu^-$ final state, in addition to the increased required statistics may disrupt this program.

With a plethora of statistics the complete angular distribution can be obtained as shown in Fig. 5. Here we compare Monte Carlo generated data for a Z' with a zero forward-backward asymmetry with both the flat distribution expected in the spin-0 case, and the $\sim 1 + z^2$ distribution ($z = \cos\theta$) of spin-1 exchange. We

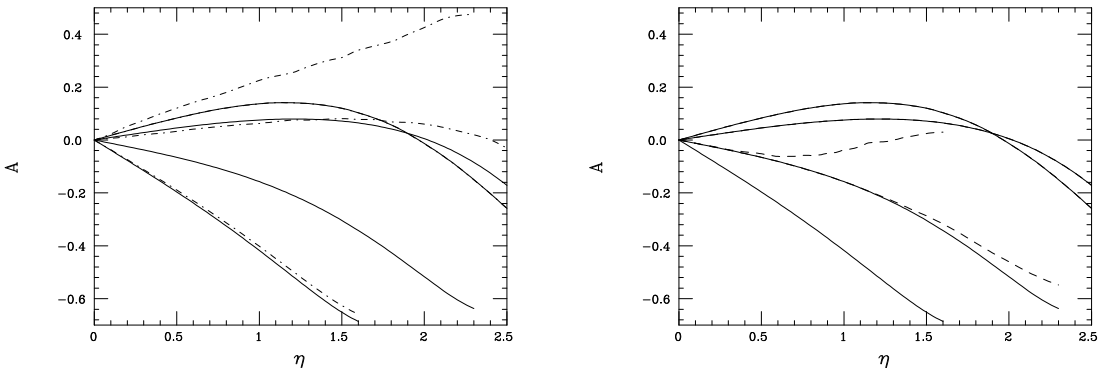

FIGURE 6. The lepton charge asymmetry in the charged current Drell-Yan production channel at the 2 TeV Tevatron for the SM (solid curves) and with 250(700) GeV $\tilde{\ell}$ exchange (the dash-dotted and dashed curves) assuming $\lambda, \lambda' = 0.15$. From top to bottom in the center of the figure, the SM curves correspond to M_T bins of 50-100, 100-200, 200-400 and > 400 GeV, respectively.

ignore complications due to possible acceptance losses arising from rapidity cuts in the forward and backward directions. Such a distribution has been measured by CDF both on and above the SM Z resonance [45]. This analysis indicates that of order ~ 1000 events are required to make a clean measurement, which is a sample approximately 100 times larger than that required for discovery. Although such measurements would be conclusive as to the identity of the spin of the resonance, the required statistics results in a significant loss in the mass range over which it can be performed. In the example discussed above where the slepton search reach was 700 GeV we find that the angular distribution could only be determined for masses below ~ 400 GeV assuming the same X value.

Angular distributions cannot be used to separate between possible $\tilde{\ell}$ and W' production in the charged current channel due to the missing energy in the event. However, there are two other useful observables in this case. First, is the transverse mass (M_T) distribution associated with the new Jacobian peak region where interference with the SM amplitude would occur for W', but not slepton, production. This test is unfortunately far more difficult to perform than in the neutral current channel again due to the missing energy as well as mass smearing. A second possibility is to examine the leptonic charge asymmetry, $A(\eta)$, for the electrons or muons in the final state as a function of their rapidity, where

$$A(\eta) \equiv \frac{dN_+/d\eta - dN_-/d\eta}{dN_+/d\eta + dN_-/d\eta}\,, \tag{10}$$

where $N_\pm$ is the number of positively/negatively charged electrons of a given rapidity, η. In the SM, the charge asymmetry is sensitive to the ratio of u-quark to d-quark parton densities and the $V-A$ nature of the W production and decay. [46] Since the coupling structure of the SM W has been well-measured, any deviations in this asymmetry within the M_T bin surrounding the W mass have been attributed to modifications in the parton distributions. Here, we are more interested in events with larger values of M_T. Note that $A(-\eta) = -A(\eta)$ if CP is conserved (which we assume) so that we will only need to deal with $\eta \geq 0$ in the following discussion.

Figure 6 displays the lepton charge asymmetry within four M_T bins, corresponding to $50 < M_T < 100$ GeV, $100 < M_T < 200$ GeV, $200 < M_T < 400$ GeV and $400 < M_T < 1800$ GeV, for the SM and with a 250(700) GeV $\tilde{\ell}$ with, for purposes of demonstration, $\lambda, \lambda' = 0.15$. In particular, the lepton charge asymmetry can be significantly altered for larger values of M_T in the bins associated with the new Jacobian peak. Note, however, that there is essentially no deviation in the asymmetry in the transverse mass bin associated with the SM W peak, $50 < M_T < 100$ GeV, so that this M_T region can still be used for determination of the parton densities. The figure also shows that the presence of the $\tilde{\ell}$ tends to drive the asymmetry to smaller absolute values as perhaps might be expected due to the presence of a spin-0 resonance.

Figure 7 presents the corresponding modifications in the leptonic charge asymmetry due to an 800 GeV W' with either purely left-handed(LH) or purely right-handed(RH) fermionic couplings. Note that the W' with purely RH couplings, unlike the LH W', does not interfere with the SM amplitude, similar to the case of $\tilde{\ell}$ production. We see that the deviation in the asymmetry due to either type of W' is very different than that

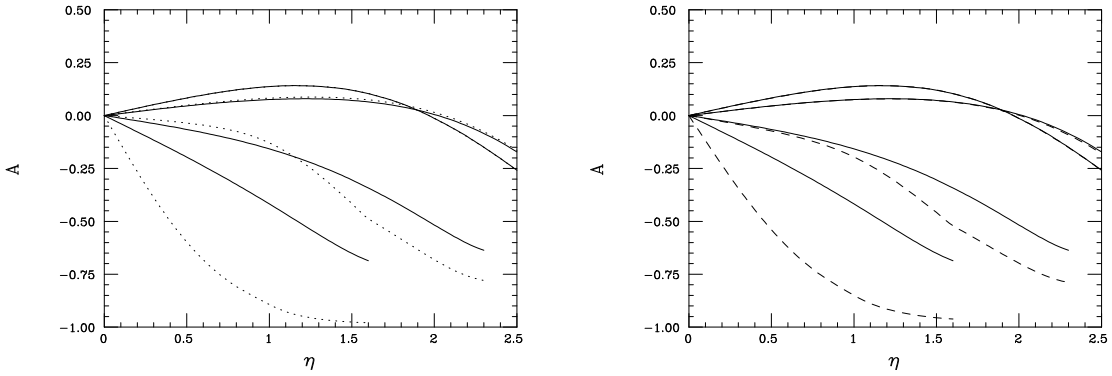

FIGURE 7. Same as the previous figure but now for the case of a 800 GeV W' with purely left-handed(left panel) or purely right-handed(right panel) couplings.

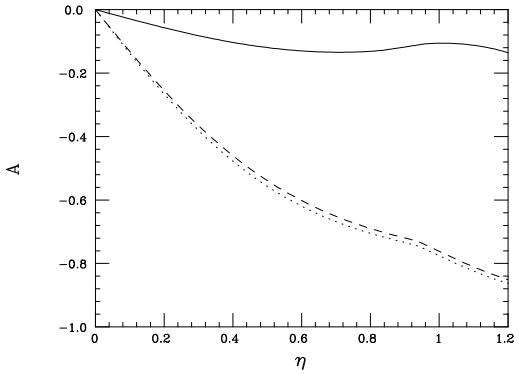

FIGURE 8. Direct comparison of the charge asymmetry induced by a 800 GeV $\tilde{\ell}$(solid) and a left- or right-handed W'(dot and dash) of the same mass, taking $600 < M_T < 900$ GeV. The assumed values of the Yukawa couplings are as in the earlier figure.

for a slepton. In the W' case, the magnitude of the asymmetry is substantially increased for both left- and right-handed couplings and these two cases are themselves potentially distinguishable by using the data in the M_T bin below, but not containing, the Jacobian peak.

The M_T bins we have taken in this analysis are rather broad. We might expect that if the width of the M_T bin around the W' or slepton Jacobian peak is compressed then the purity of the resonant contribution will be increased resulting in a better separation of the two cases (at the price of reduced statistics). These expectations are realized in Fig. 8 which shows a more direct comparison of the lepton charge asymmetries for a $\tilde{\ell}$ and W' of the same mass (800 GeV) taking the width of the M_T bin surrounding the Jacobian peak to be only 300 GeV. However, the left- and right-handed W' possibilities are no longer separable since this requires interference with the SM.

Deviations in the leptonic charge asymmetry can also be used to probe indirectly for the exchange of $\tilde{\ell}$ through $\not{R}_p$ couplings. To demonstrate this, we fix the $\tilde{\ell}$ width to mass ratio to be $\Gamma/m = 0.004$ and subdivide each of the four M_T bins discussed above into rapidity intervals of $\Delta\eta = 0.1$. For a fixed slepton mass and integrated luminosity we generate Monte Carlo data for various values of the Yukawa couplings and perform a χ^2 analysis to obtain the sensitivity to the product $\lambda\lambda'$. The 95% C.L. search reach from this analysis is shown in Fig.9 where it is clear that the reach obtained in this manner is rather modest.

6 Summary

The above analysis shows that resonant s-channel slepton production with subsequent decay into purely leptonic or dijet final states via $\not{R}_p$ couplings is observable in hadronic collisions over a wide range of parameters. If this signature is observed, we have demonstrated that the leptonic angular distributions and the lepton charge

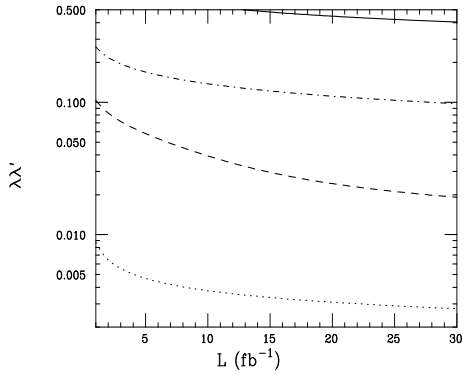

FIGURE 9. Search reach for $\tilde{\ell}$ exchange as a function of the integrated luminosity assuming $\Gamma/m = 0.004$ for masses of 1500, 1000, 750 and 250 GeV (from top to bottom).

TABLE 2. Summary of the Background Simulation

Process	Cross section before Cuts /nb	No. of Events simulated	Expected No. of Events after cuts, for $2\,\mathrm{fb}^{-1}$ luminosity
$b\bar{b}$ mixing	$(9.3 \pm 2.3) \times 10^4$	8.3×10^6	0.12 ± 0.12
$t\bar{t}$	6.81 ± 0.31	2.0×10^5	0.02 ± 0.02
single top	1.55 ± 0.12	3.5×10^4	0.00 ± 0.03
Total			0.14 ± 0.13

asymmetry can be successfully used to distinguish slepton resonances from those associated with new gauge bosons. This process provides a clean and powerful probe of $R\!\!\!/_p$ supersymmetric parameter space.

IV R-PARITY CONSERVING DECAY OF THE SLEPTON

H. Dreiner, M. Seymour, P. Richardson

In this section we discuss the resonant charged slepton production via the operator $L_i Q_j D^c_k$ followed by the decay to the neutralino decay as shown in (5)g.

$$u_j \overline{d}_k \to \tilde{\ell}^+_i \to \ell^+_i + \chi^0_n. \tag{11}$$

The neutralino in turn then decays via the same $R\!\!\!/_p$-operator $\mathrm{L_i Q_j \overline{D}_k}$,

$$\tilde{\chi}^0 \to \{\ell^-_\mathrm{i} + \mathrm{u_j} + \overline{\mathrm{d}}_\mathrm{k};\ \nu_\mathrm{i} + \mathrm{d_j} + \overline{\mathrm{d}}_\mathrm{k}\}. \tag{12}$$

Since the neutralino is a Majorana fermion it can also decay to the charge conjugate final states, with equal probability. In spirit, this is similar to the HERA process considered in [47,48].

The tree-level Feynman diagrams for the slepton production and the neutralino decay are shown in Fig. 1 and Fig. 2, respectively. Due to the Majorana nature of the neutralino, we have a signature of two like-sign charged leptons. In the following we shall consider only electrons or muons, *i.e.* we focus on the operators $\mathrm{L_e Q_j \overline{D}_k}$ and $\mathrm{L_\mu Q_j \overline{D}_k}$. We expect these leptons to have high transverse momentum, p_T, and be well isolated whereas the leptons from the Standard Model backgrounds have lower p_T and are also poorly isolated. We therefore hope that this signature can be seen above the background if we apply isolation and p_T cuts.

A Backgrounds

In the following we combine the backgrounds for both electrons and muons. The main backgrounds to this like-sign dilepton signature are as follows

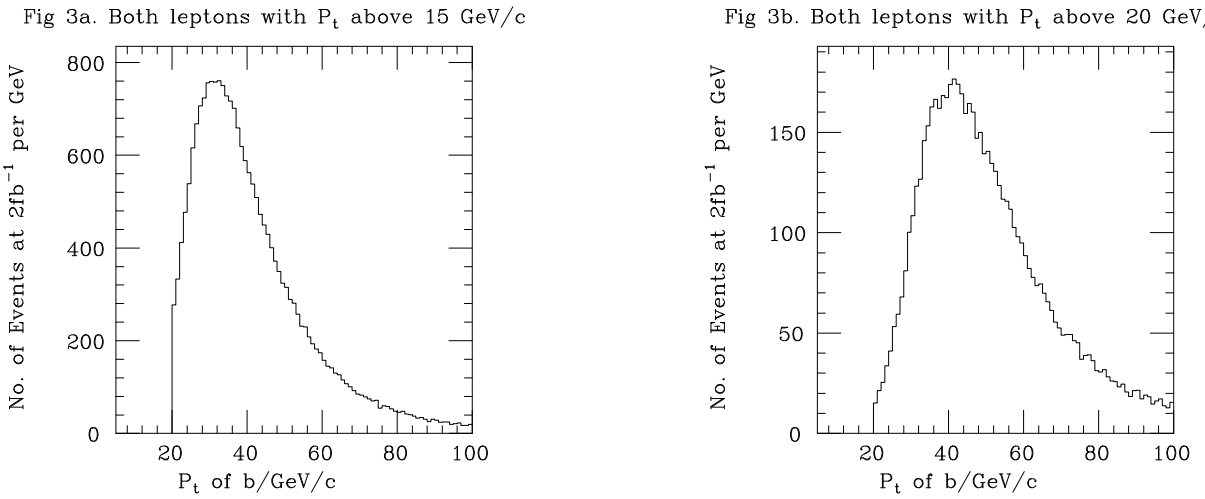

FIGURE 10. Effect of the Parton-Level Cuts.

1. $\underline{b\bar{b}\text{ production}}$ followed by the production of at least one $B^0_{d,s}$ meson, which undergoes mixing. If the two b-quarks in the event decay semi-leptonically this gives two like-sign charged leptons.
2. $\underline{t\bar{t}\text{ production}}$ followed by $t \to W^+b \to e^+\bar{\nu_e}b$, and $\bar{t} \to W^-\bar{b} \to q\bar{q}\bar{b} \to q\bar{q}W^+\bar{c} \to q\bar{q}e^+\bar{\nu_e}\bar{c}$.
3. $\underline{\text{Single top production}}$ (s and t channel) followed by semi-leptonic decays of the top and the B-meson produced after hadronization.
4. $\underline{\text{Non-physics backgrounds}}$ from fake leptons and charge misidentification. There are also backgrounds due to the production of weak boson pairs, *i.e.* WZ and ZZ, where at least one of the charged leptons is not detected [49]. These require a full simulation including the detector. We do not consider them here.

We use HERWIG 6.0, [50–52], to simulate these background processes. The program includes the computation of the supersymmetric spectrum and the MSSM decay branching ratios from the ISASUSY program [53]. Due to the high cross section for the production of $b\bar{b}$ it was necessary to impose a parton-level cut of 20 GeV on the p_T of the b and $\bar{b}$ to enable us to simulate a sufficient number of events. In Fig. 10 we show the distribution of events (using the full Monte Carlo simulation) as a function of the (parton-level) p_T of the bottom quark for two different values of the lepton p_T cut. We did not simulate any events for which the p_T of the bottom quark was below 20 GeV since the cross section is too large. If we extrapolate using Figs. 10a, b to lower b-quark p_T we can see that for a lepton p_T cut of 20 GeV, Fig. 10b, our approximation should be good, *i.e.* we expect the area under the curve for $p_T(b) < 20\,\text{GeV}$ to be negligible. For $p_T(\ell) > 15\,\text{GeV}$, Fig. 10a, we would still expect a significant number of events at $15\,\text{GeV} < p_T(b) < 20\,\text{GeV}$. Besides the parton-level cut, we forced the B-mesons to decay semi-leptonically. This means we neglect the production of leptons from the decay of charmed mesons which should also be a good approximation as we expect the leptons produced from these decays to be poorly isolated.

Figure 11 displays the effect of the lepton isolation cut on the $b\bar{b}$ background for two different values. The effect of the isolation cut on the $t\bar{t}$ and single top backgrounds is shown in Fig. 12. As can be seen in Figs. 11, 12, by imposing an isolation cut of 5 GeV and a cut on the p_T of the leptons of 20 GeV the background can be almost eliminated. Table 2 shows the backgrounds with a p_T cut on the leptons of 20 GeV and an isolation cut of 5 GeV. We have used the leading-order cross section for the $b\bar{b}$ and single top backgrounds and the next-to-leading order cross section, with next-to-leading-log resummation, from [54] for the $t\bar{t}$ cross section. In both cases the error on the cross section is the effect of varying the scale between half and twice the hard scale, and the error on the number of events is the error in the cross section and the statistical error from the simulation added in quadrature. Realistically we cannot reduce these statistical errors due to the large number of events we would need to simulate. We have implemented the full hadronization using HERWIG 6.0.

With these cuts and using Poisson statistics, a 5σ fluctuation of the total background corresponds to 4 events with an integrated luminosity of $2\,\text{fb}^{-1}$. Hence we consider 4 signal events to be sufficient for a discovery of the new $\not{R}_p$ signal process.

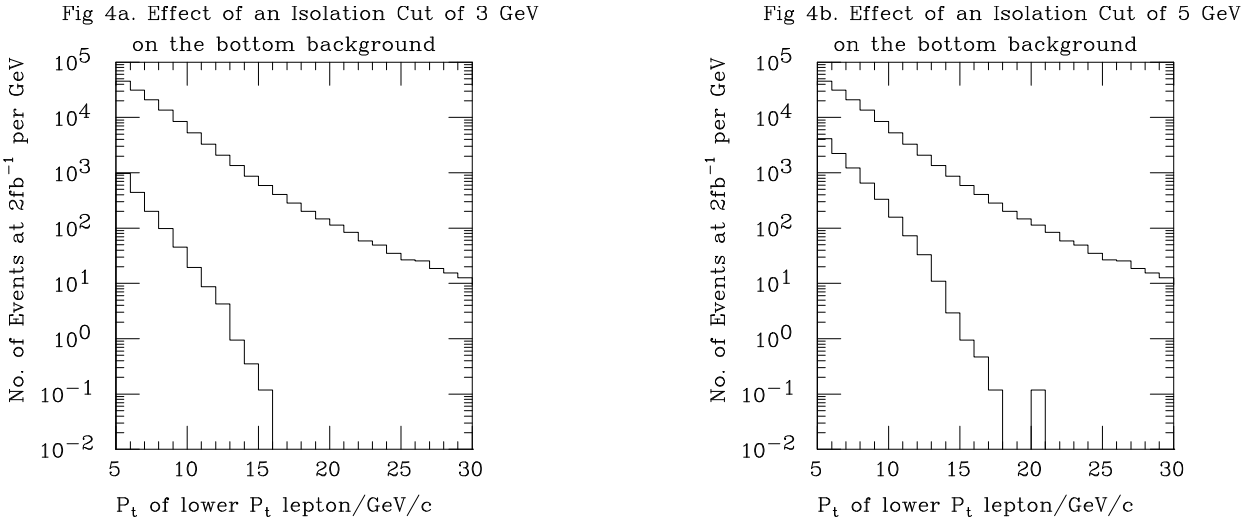

FIGURE 11. Effect of the lepton isolation cut on the $b\bar{b}$ background. The upper curve is the full $b\bar{b}$ background and the lower curve is obtained after imposing the isolation cut.

B Signal

To simulate the signal and the effect of the cuts, we modified HERWIG 6.0, [50–52], to include the production process, the MSSM decay of the slepton, and the $\not{R}_p$ decay of the neutralino. The decay rate of the neutralino and its branching ratios were calculated in the code and a matrix element for the neutralino decay [55,56] was implemented in the Monte Carlo simulation.

We use the program to estimate the acceptance of the signal process, *i.e.* the fraction of the like-sign dilepton events which pass the cuts multiplied by the branching ratio to give a like-sign dilepton event. Fig. 13 shows the acceptance for two different SUGRA points, with an isolation cut on the leptons of 5 GeV and a cut $p_{\rm T}(\ell) > 20\,{\rm GeV}$. As can be seen in Fig. 13b, the acceptance drops in two regions. For lower values of M_0, the slepton is not much heavier than the neutralino. The charged lepton from the decay of the slepton is then quite soft and gets rejected by the $p_{\rm T}$ cut. For large values of M_0 the slepton is much heavier than the neutralino. The neutralino then gets a significant boost from the slepton decay. The neutralino decay products are folded forward in the direction of this boost causing the event to be rejected by the lepton isolation cut.

To estimate the acceptance properly we need to run a scan of the SUGRA parameter space using the Monte Carlo event generator. This still remains to be done. To give some idea of what range of couplings and masses we may be able to probe instead we assume an acceptance of 10% using the same cuts as before. We can then estimate the range of couplings which may be accessible.

As can be seen in Figs. 14, 15 the production cross section for $\lambda'_{211} = 10^{-2}$ is sufficient to produce a signal which is more than 5σ above the background for large regions of the SUGRA parameter space. In some regions where the neutralinos become Higgsino-like the cross section drops. The cross section also drops as we approach the region where the neutralino is heavier than the slepton and the resonance becomes inaccessible.

We focused on the coupling λ'_{211} because the experimental bound on λ'_{111} from neutrinoless double beta decay is very strict, [57,1], as discussed in Sect. II A. The bound on λ'_{111} weakens as the squark mass squared and for squark masses above about 300 GeV (which we expect in the SUGRA scenario for the heavier slepton masses) $\lambda'_{111} \approx 10^{-2}$ is experimentally allowed and our analysis thus applies for this case as well. $\lambda'_{211} \approx 10^{-2}$ is well within the present experimental bounds [1].

In these figures we see that we are sensitive to slepton masses up to 300 GeV for couplings of 10^{-2}. The production cross section scales with the square of the coupling. For slepton masses around 100 GeV, just above the LEP limits, we can thus probe couplings down to about 2×10^{-3}.

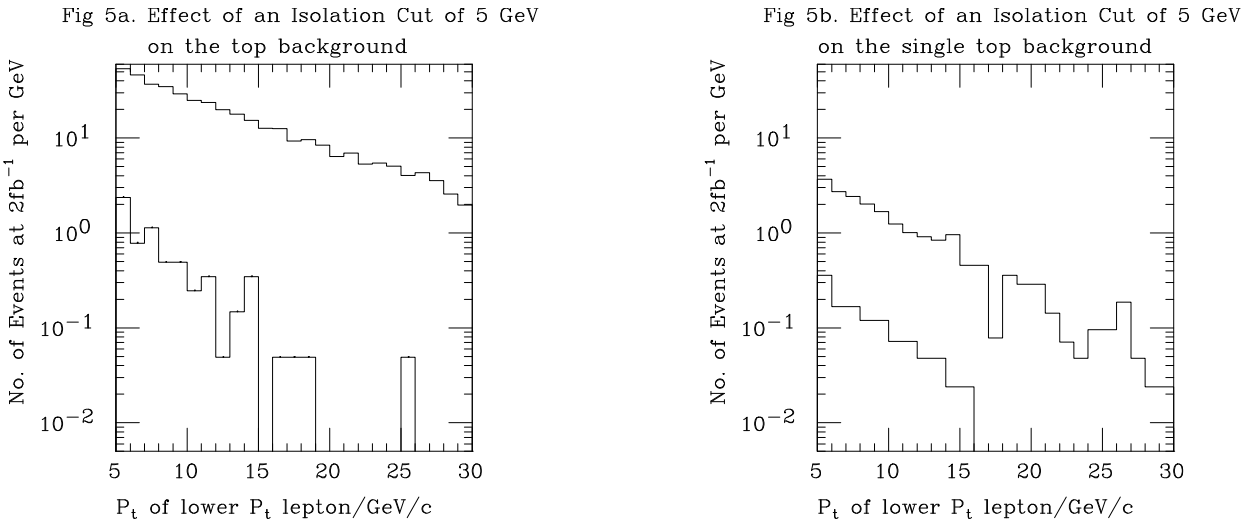

FIGURE 12. Effect of the Isolation Cut on the $t\bar{t}$ and single top Backgrounds

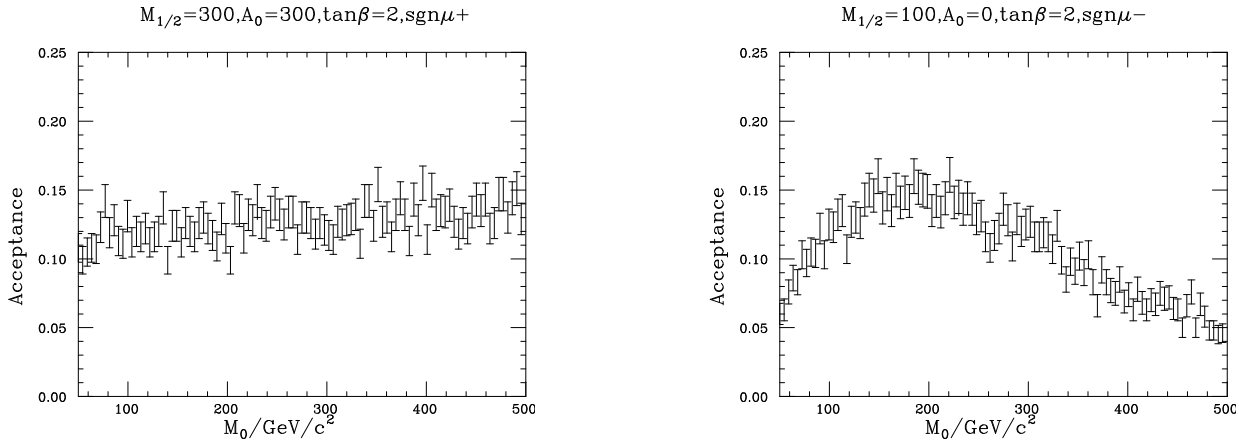

FIGURE 13. Acceptance from Monte Carlo Simulation for two different SUGRA points.

C Conclusion

We have performed an analysis of the physics background for like-sign dilepton production at Run II and find that with an integrated luminosity of $2\,\mathrm{fb}^{-1}$, a cut on the transverse momentum of the leptons of 20 GeV and an isolation cut of 5 GeV the background is 0.14 ± 0.13 events. This means that 4 signal events would correspond to a 5σ discovery, although in a full experimental analysis the non-physics backgrounds must also be considered.

Using a full Monte Carlo simulation of the signal including a calculation of the neutralino decay rate, its partial widths and a matrix element in the simulation of the decay we found that the acceptance for the signal varies but for a reasonable range of parameter space is 10% or greater.

When we then look at the cross section for the production of $\tilde{\chi}^0\ell^+$ we find that we can probe $\not{R}_p$ couplings of 2×10^{-3} for slepton mass of 100 GeV and up to slepton masses of 300 GeV for $\not{R}_p$ couplings of 10^{-2}, and higher masses if the coupling is larger.

Acknowledgments: The work of P.R. is supported by PPARC, UK.

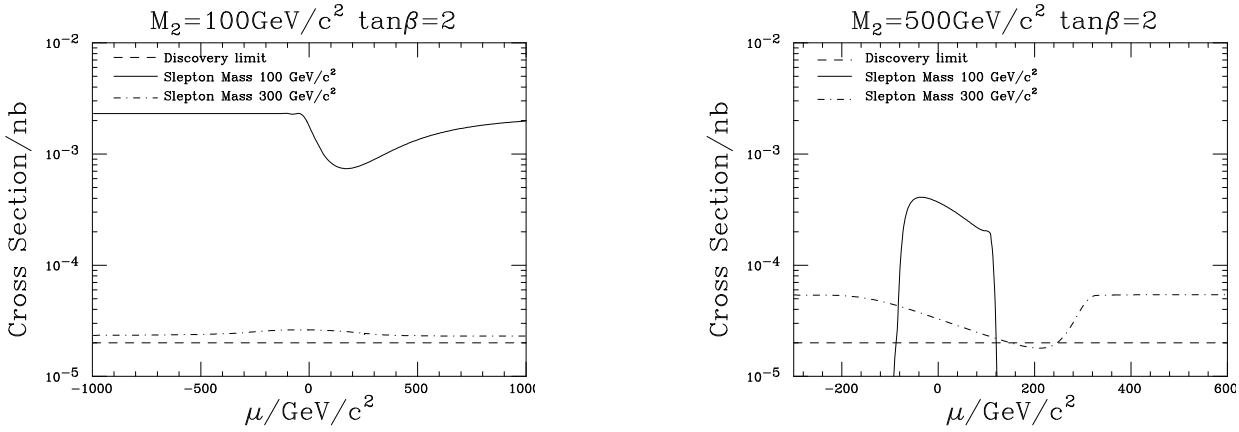

FIGURE 14. Cross section for $\tan\beta = 2$ and $\lambda'_{211} = 10^{-2}$. The long-dashed horizontal line corresponds to the discovery limit of 4 signal events for $2\,\mathrm{fb}^{-1}$. The signal cross section after cuts is given by the solid and dot-dashed curves for two slepton masses.

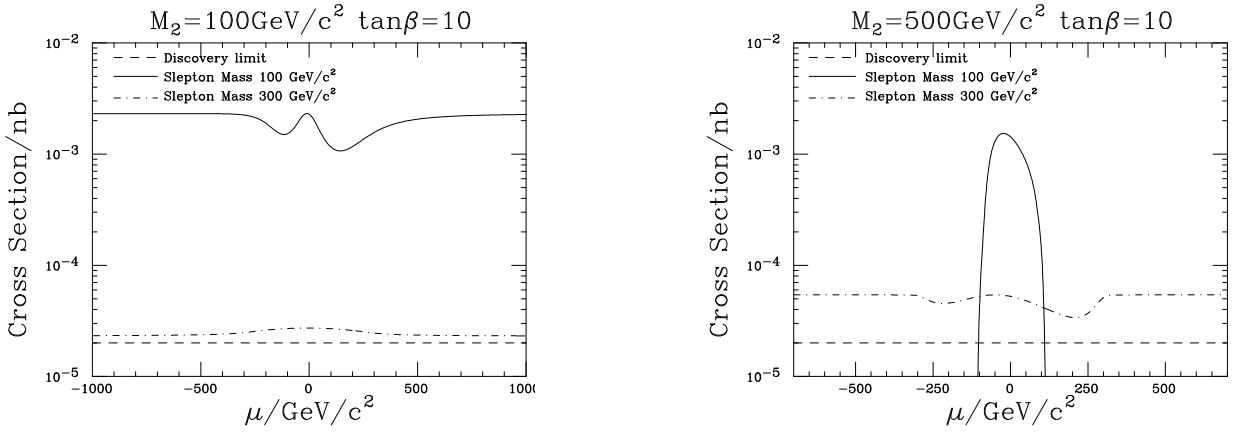

FIGURE 15. Cross section for $\tan\beta = 10$ and $\lambda'_{211} = 10^{-2}$.

V SINGLE-TOP-SQUARK PRODUCTION VIA *UDD* COUPLINGS

E.L. Berger, B. W. Harris, and Z. Sullivan

In supersymmetric extensions of the standard model, the bounds on possible R-parity-violating couplings are relatively restrictive for the first two generations of quarks and leptons, but much less so for states of the third generation (*cf.* Sect.II A. If R_p is conserved superpartners must be produced in pairs. In many models, the squarks and gluinos are relatively heavy, and therefore their pair production incurs a large phase space suppression at the energy of the Tevatron. Here, the s-channel production of a *single* squark through an $\not{R}_p$-mechanism [21] is considered. Our motivation is that the greater phase space offsets the reduced coupling strength in the production. We focus on the relatively light top squark $\widetilde{t}_1$ [58] and its subsequent R_p-*conserving* decays [59]. The R_p violation penalty is paid only once, in the initial production, and is offset by the greater phase space relative to pair production.

We choose one clean R_p-conserving decay mode, $\widetilde{t}_1 \to b\widetilde{\chi}_1^+$, with $\widetilde{\chi}_1^+ \to l^+ + \nu + \widetilde{\chi}_1^0$. Here, l is an electron or muon, and the $\widetilde{\chi}_1^+$ and $\widetilde{\chi}_1^0$ are the chargino and lowest-mass neutralino states of the MSSM. For top-squark masses in the range of 180–325 GeV, we simulate both the signal and standard model background processes and thereby show that the top squark can be discovered, or the current bound on the size of the R_p-violating

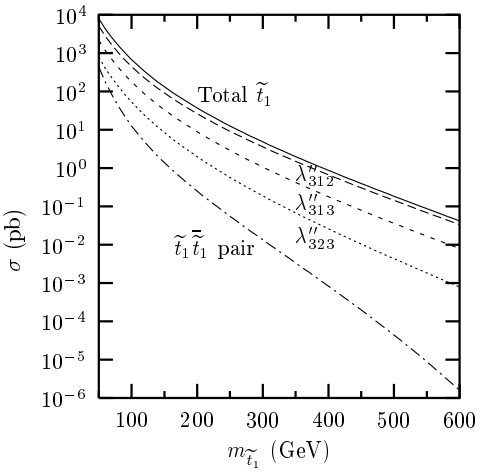

FIGURE 16. Cross section for R_p-violating production of a single top-squark at Run II of the Tevatron ($\lambda''_{3ij} = 0.1$) compared with the cross section for R_p-conserving production of pairs. Both cross sections are computed at leading order.

coupling λ''_{3ij} can be reduced by up to one order of magnitude with existing data and by two orders of magnitude at the forthcoming run II of the Fermilab Tevatron [59].

In general it is possible to have R_p-violating contributions to the MSSM superpotential of the baryon- or lepton-number violating type. However, limits on the proton decay rate severely restrict their simultaneous presence. We therefore assume the existence of a baryon-number-violating coupling only of the form [60]

$$\mathcal{W}_{\not R_p} = \lambda''_{ijk} U^c_i D^c_j D^c_k \; . \tag{13}$$

Here, U^c_i and D^c_i are right-handed-quark singlet chiral superfields, i, j, k are generation indices, and c denotes charge conjugation. For production of a right-handed top squark via an s-channel diagram $\bar{d}^j \bar{d}^k \to \widetilde{u}^i_R$ the relevant couplings are λ''_{312}, λ''_{313}, and λ''_{323}. The current best limits on these couplings come from experiments at the CERN Large Electron Positron Collider (LEP). Measurement of R_l, the partial decay width to hadrons over the partial decay width to leptons of the Z boson, limits the values of λ''_{3ij} to be less than approximately 0.5 (*cf* Sect. II A).

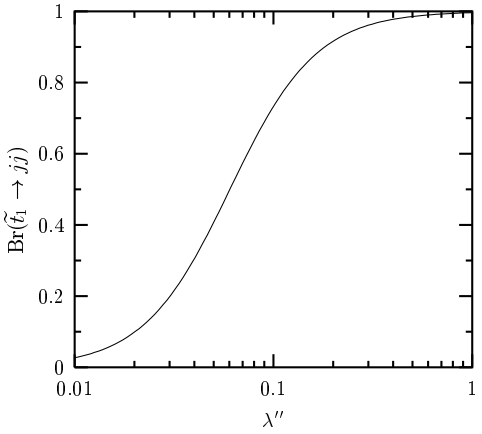

FIGURE 17. Branching ratio for the top squark to decay into two jets via the R-parity-violating coupling λ'' as a function of the coupling. The values of the SUGRA parameters are given in the text.

The colour- and spin-averaged partonic cross section for $qq' \to \bar{\widetilde{t}}_1$ is

TABLE 3. Cuts used to simulate the acceptance of the detector at the Tevatron run II, and run I (in parentheses if different). The lepton veto ($E_{Tl} < 45$ GeV) is optimized for small top-squark mass.

$\|\eta_b\| < 2$ (1)	$E_{Tb} > 40$ GeV
$\|\eta_l\| < 2.5$ (1.1)	$E_{Tl} > 15$ GeV (20 GeV)
$\|\eta_j\| < 2.5$	$E_{Tj} > 20$ GeV
$\|\Delta R_{bj}\| > 0.7$	$\|\Delta R_{jl}\| > 0.7$
$\not\!\!E_T > 20$ GeV	$E_{Tl} < 45$ GeV

$$\hat{\sigma} = \frac{2\pi}{3}|\lambda''_{3ij}|^2 \frac{\sin^2\theta_{\widetilde{t}}}{m^2_{\widetilde{t}_1}} \delta(1 - m^2_{\widetilde{t}_1}/\hat{s}) \ , \tag{14}$$

where $\sqrt{\hat{s}}$ is the partonic center of mass energy, and $\theta_{\widetilde{t}}$ relates the right- and left-handed top-squark interaction states to the mass eigenstates. The hadronic cross section depends on the following combinations of incident parton distribution functions (PDF's): $d \otimes s$, $d \otimes b$, and $s \otimes b$, where d, s, and b denote the PDF's of the down, strange, and bottom quarks, respectively. We assume $\lambda''_{312} = \lambda''_{313} = \lambda''_{323} \equiv \lambda''$. Our numerical results represent the sum of $\widetilde{t}_1$ and $\overline{\widetilde{t}}_1$ production.

The mass dependences of the cross sections for single and pair production of top squarks at the Fermilab Tevatron ($\sqrt{s} = 2$ TeV) differ significantly, as shown in Fig. 16. The curves are based on CTEQ4L leading order parton distribution functions [61] and $\lambda'' = 0.1$, an order of magnitude below the current limit. In fact, λ'' can be smaller by an additional order of magnitude and the single-top-squark cross section will still exceed that for pair production if $m_{\widetilde{t}_1} > 100$ GeV.

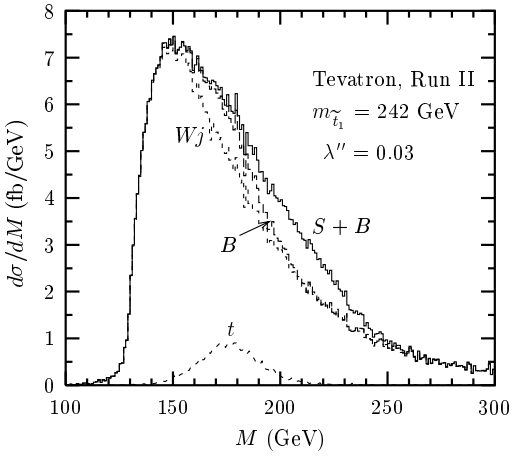

FIGURE 18. The reconstructed-mass M distribution for single-top-squark production plus background ($S+B$) at the Tevatron ($\sqrt{s} = 2$ TeV) for a top-squark mass $m_{\widetilde{t}_1} = 242$ GeV. Also shown is a decomposition of the total background (B) into it's major components, all W jet modes (Wj) and single-top-quark production (t). The coupling $\lambda'' = 0.03$ produces the minimum signal for a 5σ significance at this mass.

In the MSSM, the up-type squark $\widetilde{u}^k$ can decay into charginos and neutralinos via the two-body processes $\widetilde{u}^k \to d^k + \widetilde{\chi}^+_j$ $(j = 1, 2)$ and $\widetilde{u}^k \to u^k + \widetilde{\chi}^0_j$ $(j = 1, 2, 3, 4)$. Three body modes are possible, including $\widetilde{t}_1 \to W^+ + b + \widetilde{\chi}^0_1$, which is similar to decay into the top quark (followed by top decay to $W^+ + b$) but softer; and $\widetilde{t}_1 \to c + \widetilde{\chi}^0_j$ via a flavor-changing loop process. The squark can also decay into a gluino plus a quark if allowed kinematically.

With baryon-number-violating terms present, the top squark can also decay into quark pairs via the λ'' couplings. The branching fraction into two jets is shown in Fig. 17 for the specific SUGRA point discussed below. The branching ratio is quite insensitive to the SUGRA parameters over a wide range. If λ'' is large, the decay to quark jets dominates. However, as shown below, the R_p-conserving decay still produces a measurable and useful cross section.

For the remainder of this study, we focus on the two-body decay mode [22] $\widetilde{t}_1 \to b + \widetilde{\chi}_1^+$, with $\widetilde{\chi}^+ \to l + \nu + \widetilde{\chi}_1^0$. Here, l denotes an electron or muon, which usually comes from a W. We expect $\widetilde{\chi}_1^0$ to undergo an R_p-violating decay outside of the detector, so it is treated as stable for our purposes.

A minimal supergravity model [62] is adopted to obtain the relevant masses and decay branching fractions. We begin with common scalar and fermion masses of $m_0 = 100$ GeV and $m_{1/2} = 150$ GeV, respectively, at the GUT scale. We choose a trilinear coupling $A_0 = -300$ GeV and the ratio of the Higgs vacuum expectation values $\tan\beta = 4$. The absolute value of the Higgs mass parameter μ is fixed by electroweak symmetry breaking and is assumed positive. Superpartner masses and decay widths are calculated with ISAJET [53]. At the weak scale, $m_{\widetilde{t}_1} = 183$ GeV, $m_{\widetilde{\chi}_1^0} = 55$ GeV, and $m_{\widetilde{\chi}_1^\pm} = 103$ GeV. In order to isolate the effects of the $\not{R}_p$ sector, we vary m_0 and keep the other supersymmetric parameters fixed. Since the gaugino masses depend primarily on the choice of $m_{1/2}$, variation of m_0 allows us to vary $m_{\widetilde{t}_1}$ without any appreciable change in the masses of the decay products.

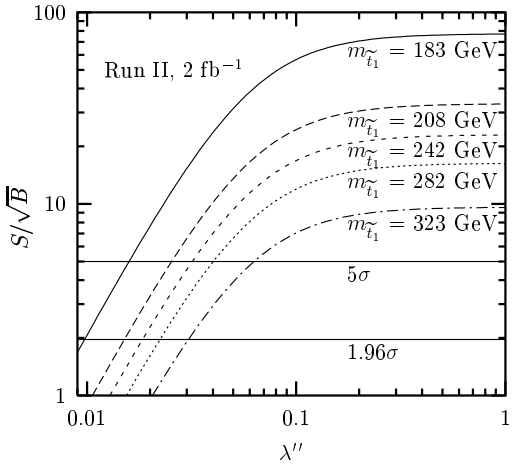

FIGURE 19. Statistical significance of the single-top-squark signal ($S/\sqrt{B}$) in run II of the Tevatron ($\sqrt{s} = 2$ TeV, 2 fb^{-1}) versus λ'' for a variety of top-squark masses.

For the four-body decay mode of interest, the signal consists of a tagged b-quark jet, a lepton, and missing transverse energy associated with the unobserved neutrino and $\widetilde{\chi}_1^0$. The dominant backgrounds, in order of importance, arise from production and decay of the standard model processes Wc, in which a W is produced in association with a charm quark c that is mistaken for a b; Wj, in which a W is produced in association with a hadronic jet that mimics a b; $Wb\bar{b}$; $Wc\bar{c}$; and single-top-quark production via Wg fusion. For these background processes, we work with tree-level matrix elements obtained from MADGRAPH [63] convolved with leading-order CTEQ4L [61] parton distribution functions, at a hard scattering scale $\mu^2 = \hat{s}$. In an experimental analysis, the Wj background will be normalized by the data. To simulate the resolution of the hadron calorimeter, we smear the jet energies with a Gaussian whose width is $\Delta E_j/E_j = 0.80/\sqrt{E_j} \oplus 0.05$ (added in quadrature).

We simulate the acceptance of the detector by using the selections listed in Table 3. The assumed coverage in rapidity for taggable b-quark jets and leptons is smaller for run I than for run II. However, the signal and background are similar in shape in these variables, and thus S/B is not sensitive to this cut. The lepton must be isolated from any jets, as defined by a cone of radius ΔR, or it is considered missed. Similarly, an isolation cut is used for the b-quark jet in order to help identify it. We assume a b-tagging efficiency of 60% (50% for run I) with a mistag rate of 15% for charm quarks and 0.5% for light quarks [43]. Missing momentum is identified with a *massless* particle whose three-momentum balances that of the b-quark and the lepton.

As expected from the primary decay, $\widetilde{t}_1 \to b + \widetilde{\chi}_1^+$, the distribution in the transverse energy E_T of the b

quark is peaked sharply near the maximum value allowed kinematically. The spectrum of the background b quark is soft, and thus we impose a hard cut ($E_{Tb} > 40$ GeV) on the minimum E_T of the b-quark jet. For larger values of $m_{\tilde{t}_1}$ this cut would be optimized by raising the minimum E_{Tb}. The b-jet becomes too soft to be detected if $m_{\tilde{t}_1} \leq m_{\tilde{\chi}_1} + E_T^{\rm cut}$. This contributes to a lower limit on $m_{\tilde{t}_1}$ below which our proposed search mode is not useful.

The background from single-top-*quark* production will produce a peak in any mass reconstruction. We utilize the fact that single top-quarks are often produced with extra hard jets, and we impose a "jet veto". We require that there be no hard jets in the hadron calorimeter ($E_{Tj} > 20$ GeV, $|\eta| < 2.5$), beyond the one that is b-tagged. After the jet veto, the remaining background is due almost entirely to misidentified charm and light-quark jets from Wc and Wj production. The transverse energy of the lepton tends to be relatively soft for the signal at low $m_{\tilde{t}_1}$, whereas it peaks around 40 GeV when it comes from the W in the background. A cut to remove hard leptons, with $E_{Tl} > 45$ GeV, reduces the background by a factor of 2 with little effect on the signal at low masses. The final significance for the signal at run II is barely changed by this "lepton veto", but it is especially helpful for the run I data.

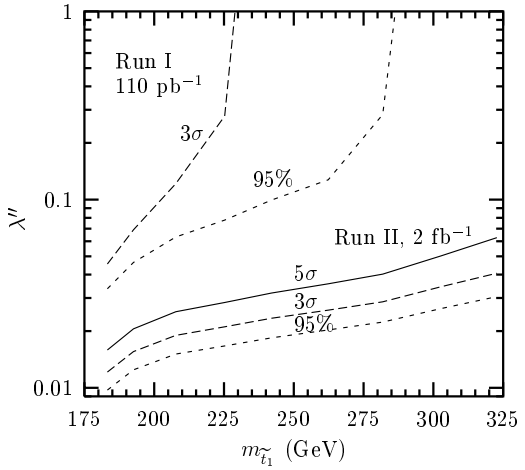

FIGURE 20. Lower limits on discovery ($S/\sqrt{B} = 5$), evidence ($S/\sqrt{B} = 3$), and 95% confidence-level exclusion ($S/\sqrt{B} = 1.96$) for λ'' versus top-squark mass in Run I of the Tevatron ($\sqrt{s} = 1.8$ TeV, 110 pb^{-1}), and in Run II ($\sqrt{S} = 2$ TeV, 2 fb^{-1}).

Shown in Fig. 18 is an example of the signal and background. For this case, $m_{\tilde{t}_1} = 242$ GeV and $\lambda'' = 0.03$. The mass variable is defined as $M^2 = (P_b + P_l + P_X)^2$ where the P_b and P_l are the four-momenta of the b and lepton. The four-momentum P_X is defined such that its three-momentum balances that of the b and lepton, and $P_X^2 \equiv 0$. The clearly discernible signal in Fig. 18 would constitute a discovery at the level of 5σ with an integrated luminosity of 2 fb^{-1} at $\sqrt{s} = 2$ TeV. When $m_{\tilde{t}_1}$ is reduced to 183 GeV, the signal and background spectra peak at about the same location, and sensitivity to the signal begins to be lost.

Examination of the structure of the cross section involving R_p-*conserving* decay modes reveals that as λ'' grows, the decrease in branching fraction is compensated by the increase in cross section. As depicted in Fig. 19,

$$\sigma \propto \frac{|\lambda''|^2}{|\lambda''|^2 + f(R_p)} \, , \tag{15}$$

where $f(R_P)$ is a constant times the branching fraction into R_p-conserving modes. As $\lambda'' \to \infty$, the cross section goes to a constant; whereas, when $\lambda'' \to 0$ the cross section decreases as $|\lambda''|^2$. The relationship $S/\sqrt{B} \propto |\lambda''|^2/\sqrt{B}$, valid for small λ'', implies a lower limit on the values of λ'' that can be probed. On the other hand, this relationship highlights an insensitivity to variations in the estimate of the background.

In Fig. 20, we show the reach in λ'' for $180 < m_{\tilde{t}_1} < 325$ GeV. With an integrated luminosity of 2 fb^{-1} at $\sqrt{S} = 2$ TeV, discovery at the level of 5σ is possible provided that $\lambda'' > 0.02$–0.05. Otherwise, a 95% confidence

level exclusion can be set for $\lambda'' > 0.01$–0.03. For the lower integrated luminosity and energy of the existing Run I data, values of $\lambda'' > 0.03$–0.2 can be excluded at the 95% confidence level if $m_{\tilde{t}_1}$ =180–285 GeV.

We conclude that, as long as the R_p-conserving decay $\widetilde{t}_1 \to b\widetilde{\chi}_1^+ \to l\nu\widetilde{\chi}_1^0$ is allowed, it should be possible to discover the top squark or to reduce the lower limit on λ'' by two orders of magnitude at Run II of the Fermilab Tevatron, for $180 < m_{\tilde{t}_1} < 325$ GeV and $\lambda''_{3ij} > 0.02$–0.05. Existing data from Run I of the Tevatron should allow a reduction of the limit on λ'' by an order of magnitude. With such a reduction, one can establish that R_p-violating decay is unlikely and rule out most of the possible influence of the top squark on single-top-quark production and decay.

This work was supported by the U. S. Department of Energy, High Energy Physics Division, under Contract No. W-31-109-Eng-38.

PART 2: SParticle Pair Production

VI GLUINO AND SQUARK PAIR PRODUCTION WITH LEPTONIC DECAYS

M. Chertok

CDF has performed searches for squark and gluino production followed by $\not{R}_p$-decays using data taken with the Run I detector [64]. Upgrades of both the detector and Tevatron are currently underway [65]. These will provide substantial enhancements for these and other searches in Run II, scheduled to begin in 2000. During this run, CDF II will collect roughly 2 fb^{-1} of data at $\sqrt{s} = 2$ TeV, corresponding to twenty times the present statistics. The 10% increase in energy corresponds to a 40% increase in the $t\overline{t}$ yield, and similarly will aid new phenomena searches.

A $\not{R}_p$ Decays via LQD^c: Di-Lepton Events

Events with a positron and a jet at high Q^2 values, detected at the HERA experiments [33], have sparked interest in $\not{R}_p$ since [34] such events can be explained by the production and decay of a charm squark ($\tilde{c}_L$): $e^+ + d \to \tilde{c}_L \to e^+ + d$, where R_p is violated at both vertices. For this scenario, $\tilde{c}_L$ with mass $M(\tilde{c}_L) \simeq 200$ GeV/c^2 is the preferred squark flavor, because its associated coupling λ'_{121} [66,67] is less constrained by experiment than the others.

We test two $\not{R}_p$ processes that involve the same λ'_{121} coupling [25]:

$$p\overline{p} \to \tilde{g}\tilde{g} \to (c\,\tilde{c}_L)\,(c\,\tilde{c}_L) \;\Rightarrow c\,(e^{\pm}d)\,c\,(e^{\pm}d) \tag{16}$$

$$p\overline{p} \to \tilde{q}\overline{\tilde{q}} \to (q\tilde{\chi}_1^0)\,(\bar{q}\tilde{\chi}_1^0) \;\Rightarrow q\,(dce^{\pm})\,\bar{q}\,(dce^{\pm}) \tag{17}$$

The first we denote the "charm squark analysis" and the second the "neutralino analysis". Here, the $\not{R}_p$ decays are indicated by "$\Rightarrow$." For process (16) we assume $M(\tilde{g}) > M(\tilde{c}_L) = 200$ GeV/c^2. The masses of the other squarks are given in a MSSM scenario in Ref. [66]. For process (17), we consider $\tilde{q}\overline{\tilde{q}}$ production (5 degenerate squark flavors) and $\tilde{t}_1\overline{\tilde{t}}_1$ production separately. We also make the mass assumptions: $M(\tilde{\chi}_1^{\pm}) > M(\tilde{q}) > M(\tilde{\chi}_1^0)$, $M(\tilde{\chi}_1^{\pm}) \approx 2\,M(\tilde{\chi}_1^0)$, and $M(\tilde{\chi}_1^{\pm}) > M(\tilde{t}_1) - M(b)$, where the first relation suppresses $\tilde{q} \to \tilde{\chi}_1^{\pm}$, the second relation arises from gaugino mass unification, and the third ensures that $Br(\tilde{t}_1 \to c\tilde{\chi}_1^0) = 100\%$ for $M(\tilde{t}_1) < M(t)$. Given the Majorana nature of the gluino and neutralino, reactions (16) and (17) yield like-sign (LS) and opposite-sign (OS) dielectrons with equal probability. Since LS dilepton events have the benefit of small SM backgrounds, we search for events with LS electrons plus two or more jets.

This analysis requires at least two electrons with $E_T > 15$ GeV in the central electromagnetic calorimeter. The η-ϕ separation $\Delta R_{ee} \equiv \sqrt{(\Delta\phi)^2 + (\Delta\eta)^2}$ between two electrons must be greater than 0.4. Each electron must pass an isolation cut which requires the total calorimeter E_T in an η-ϕ cone of radius $\Delta R = 0.4$ around the electron, excluding the electron E_T, to be less than 4 GeV. Jets are identified in the calorimeter using cone size $\Delta R = 0.7$ for clustering and in the range $|\eta_j| < 2.4$. There must be at least two jets with $E_T > 15$ GeV, $\Delta R_{jj} > 0.7$, and $\Delta R_{ej} > 0.7$. We further require no significant $\not\!\!E_T$ in the event: $\not\!\!E_T/\sqrt{\sum E_T} < 5\ GeV^{1/2}$. No

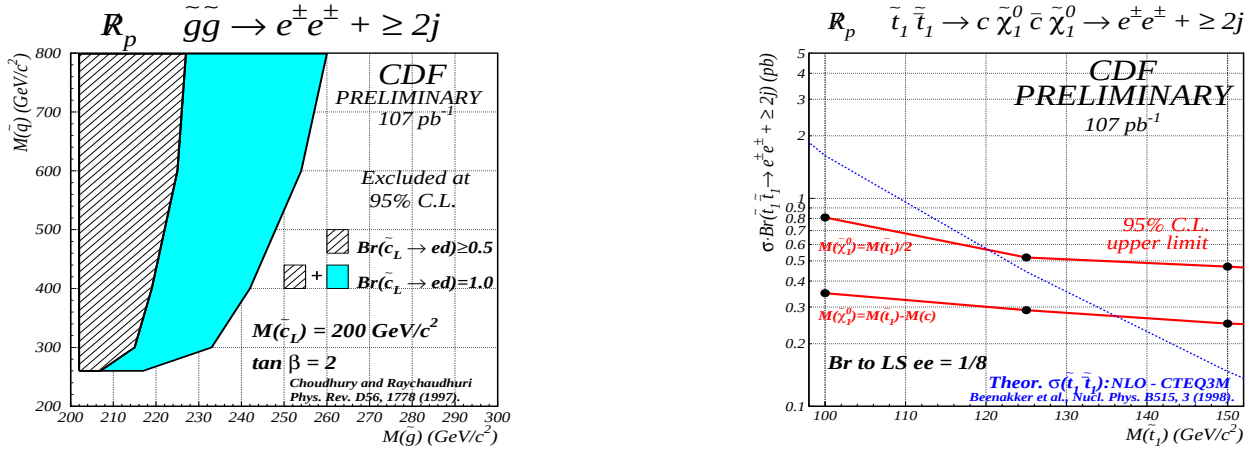

FIGURE 21. Exclusion regions in the $M(\tilde{q})$-$M(\tilde{g})$ plane (left) and upper limits on cross section times branching ratio for $\tilde{t}_1\bar{\tilde{t}}_1$ production (right).

LS ee events survive our selection. The remaining 166 OS ee events are consistent with expected contributions from SM processes, notably Drell-Yan production of dielectrons.

Event acceptances are calculated using Monte Carlo samples generated with ISAJET, CTEQ3L parton distribution functions, and passed through the CDF detector simulation program. SM backgrounds for this search, $t\bar{t}$ and $b\bar{b}/c\bar{c}$ production, are small. We find the total background in 107 pb^{-1} is consistent with zero events. We set limits on the cross section times branching ratio for the two processes under study. For the charm squark analysis, the event acceptance is a very weak function of $M(\tilde{g})$ in the range of 16.0% to 16.6%; we include a 10% systematic uncertainty (dominated by the uncertainty on the integrated luminosity), and exclude $\sigma \cdot Br \geq 0.18$ pb independent of $M(\tilde{g})$. In Figure 21 we plot the results from the charm squark analysis in the gluino-squark mass plane. Contours are shown for two values of the branching ratio $Br(\tilde{c}_L \to ed)$, where we have compared our results to the NLO $\tilde{g}\tilde{g}$ production cross section multiplied by the branching ratio to LS ee from Ref. [67].

For the neutralino analysis, the acceptance is determined for each squark and neutralino mass pair and ranges from 3.7% to 15.2%. We obtain $\sigma \cdot Br$ limits which range as a function of the squark mass from 0.81 pb to 0.26 pb for a light neutralino, and from 0.35 pb to 0.20 pb for a heavy neutralino. Figure 21 shows the results for the neutralino analysis for the case of $\tilde{t}_1\bar{\tilde{t}}_1$ production. Plotted are our 95% C.L. upper limits along with the cross section times branching ratio versus $M(\tilde{t}_1)$ from the NLO prediction. The branching ratio $Br(\tilde{t}_1 \to c\,\tilde{\chi}_1^0)$ is taken to be 1.0 We also assume $Br(\tilde{\chi}_1^0 \to q\overline{q}'e) = Br(\tilde{\chi}_1^0 \to q\overline{q}'\nu) = 1/2$, which need not be the case [47]. Since each neutralino decays to e^+ or e^- with equal probability, the branching ratio to LS ee is 1/8. This analysis excludes $M(\tilde{t}_1)$ below 120 (135) GeV/c^2 for a light (heavy) neutralino. The results for the neutralino analysis for the case of five degenerate $\tilde{q}\bar{\tilde{q}}$ production are displayed in Figure 22. Again, plotted is our cross section times branching ratio limit for two neutralino masses, along with the NLO prediction which includes a gluino mass dependent t-channel contribution to the cross section. Thus, we set gluino and neutralino mass-dependent lower limits on the degenerate squark mass in the range from 200 to 260 GeV/c^2.

We include a Run II projection for this search in Figure 22 which folds in the increased cross section at $\sqrt{s} = 2$ TeV along with the ratio of the integrated luminosities. Assuming event selection and background levels similar to those in Run I, this search will be sensitive to squark masses up to 380 GeV/c^2. The addition of the muon channel will further enhance the reach, as will the improved lepton identification in Run II.

B R_p Decays via LLE^c: Multilepton Events

If we now assume one of the LLE^c operators is non-zero, the LSP decays as in Eq.(8)a. For the case of supersymmetric pair production as in Eq.(7), followed by the cascade decay to the LSP, we then expect events with extra leptons. CDF has an analysis underway that examines $\lambda_{121} \neq 0$ [68]. As in [31], all production processes (except scalar top) are considered simultaneously. The coupling λ_{121} allows two classes of processes: 1) direct decays of sleptons and sneutrinos to leptons and neutrinos, and 2), decays of charginos and neutralinos

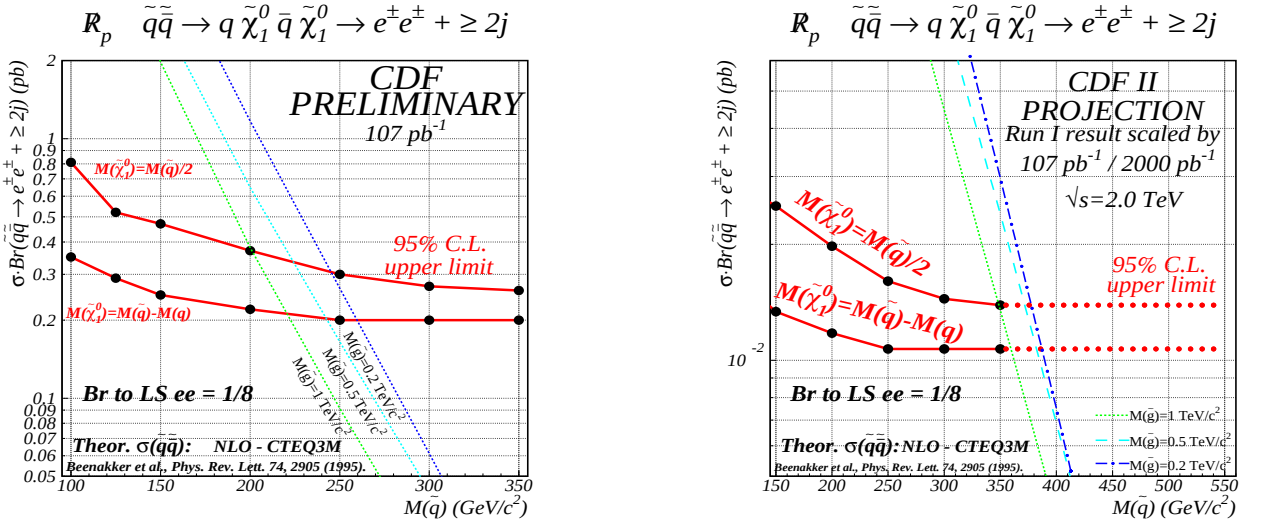

FIGURE 22. Upper limits on cross section times branching ratio for five-flavor degenerate $\tilde{q}\bar{\tilde{q}}$ production (left) and projection for Run II (right). Also shown are the NLO cross sections multiplied by a branching ratio to LS ee of 1/8 with the assumption of $Br(\tilde{q} \to q\tilde{\chi}_1^0) = 1.0$.

TABLE 4. Multilepton $R\!\!\!/_p$ search projections for Run II. The efficiencies are based on the Run I detector simulation.

M_0 (GeV/c^2)	$M_{1/2}$ (GeV/c^2)	σ (pb)	Efficiency	Four-Lepton Events
50	190	0.170	0.19	64
100	190	0.170	0.12	41
150	190	0.166	0.10	34
200	190	0.166	0.09	31
200	200	0.128	0.10	25
200	210	0.102	0.10	21
200	220	0.078	0.10	16
200	230	0.061	0.10	12
200	240	0.049	0.10	10

to leptons and neutrinos as in (8)a. It is further assumed that λ_{121} is large enough so that the $R\!\!\!/_p$ decays are prompt, *i.e.* within $\mathcal{O}(1mm)$ of the interaction point, but also that $\lambda_{121} \ll 1$. This tends to suppress both 1) and 2), except for decays of the LSP which have no competing MSSM decays. Thus, $\tilde{\chi}_1^0 \to \mu\bar{e}\nu_e$, $\bar{\mu}e\bar{\nu}_e$, $e\bar{e}\nu_\mu$ $e\bar{e}\bar{\nu}_\mu$ each with equal probability. Such events therefore contain four (or more) leptons and $\not\!\!E_T$.

Simulation of the signal is performed using ISAJET within a SUGRA framework. The mass parameters M_0 and $M_{1/2}$ are input, while the others are fixed: $A_0 = 0$, $\tan\beta = 2$, $\mathrm{sgn}\mu = -1$. The event selection requires four leptons, $\ell = (e, \mu)$, where one lepton satisfies $E_T(e) > 12\,GeV$, $|\eta_e| < 1.1$ or $p_T(\mu) > 12$ GeV/c, $|\eta_\mu| < 0.6$, while the others must satisfy $E_T(e) > 5\,GeV$, $|\eta_e| < 1.1$ or $p_T(\mu) > 5$ GeV/c, $|\eta_\mu| < 1.0$. Furthermore, the leptons must be separated by $\Delta R > 0.4$. Neither lepton isolation nor $\not\!\!E_T$ requirements are imposed. SM processes that can yield four lepton events include $t\bar{t}$, $b\bar{b}/c\bar{c}$, and Z^0Z^0 production and decay, although the rates are very low. Another background under study is that of processes containing three real leptons plus an additional fake lepton.

Projections for this search in Run II are presented in Table 4, which folds in the approximate factor of twenty in statistics and the increase in $\sqrt{s}$. The background increase to $\mathcal{O}(10)$ events in Run II could be controlled by additional cuts on $\not\!\!E_T$, jets, or lepton isolation. Improvements to the detector, for example the upgraded plug EM calorimeter, will improve the lepton identification efficiency. Such contributions are not included in this estimate.

VII D0 SEARCH FOR SUSY PAIR PRODUCTION FOLLOWED BY LQD^C LSP DECAYS

S. Banerjee, N.K. Mondal, V.S. Narasimham, N. Parua

A Physics motivation

Recent interest in R-parity violating (RPV) SUSY decay modes is motivated by the possible high-Q^2 event excess at HERA [33]. When interpretation of the excess through first-generation leptoquarks was excluded by the DØ [36] and CDF [37] experiments, it was suggested [34] that such an effect could be explained via the s-channel production of a charm or top squark decaying into the $e+jet$ final state. Both the production and the decay vertices would thereby violate R-parity. Although more recent data has not confirmed the previous event excess, interest in RPV signatures has not abated. The CDF and DØ Collaborations have recently performed searches for RPV SUSY [25,26], and have set new mass limits on the RPV SUSY particles. Both experiments focussed their searches on the λ' couplings, as motivated by the high-Q^2 HERA event excess. The results of the DØ searches are here extended to the Run II case and the expected sensitivity to the RPV couplings is discussed.

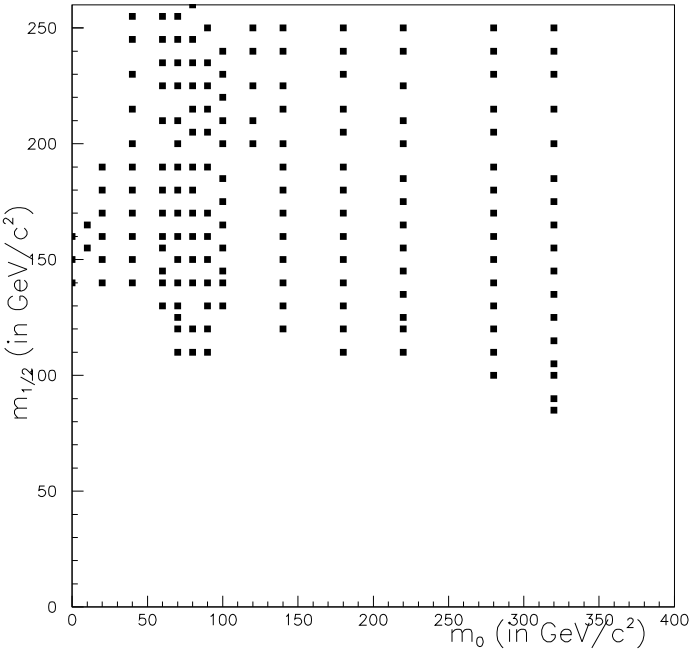

FIGURE 23. Points in the $(m_0, m_{1/2})$ SUGRA parameter space used to generate RPV events in the $ee + 4$ jets channel.

B DØ Search for RPV neutralino decays

The DØ search for RPV SUSY considered the case of neutralino LSP which decays into a lepton and two quarks due to a finite RPV λ' coupling (see Fig. 2). Both the electron and muon decay channels were considered, corresponding to what is commonly referred to as λ'_{1ij} and λ'_{2ij} couplings, respectively. The corresponding final states contain either $2e$ or 2μ and at least four accompanying jets. Unlike at HERA, this search is not sensitive to the value of the RPV coupling, as long as it is large enough so that the neutralino decays within the DØ detector. That corresponds to $\lambda' \geq 10^{-3}$, which gives a lot of room, given current indirect constraints (see Sect. II A).

TABLE 5. Efficiency × BR (%), signal cross section and the expected event yield in 2 fb^{-1} of data, at various $(m_0, m_{1/2})$ parameter space points.

m_0 (GeV)	$m_{1/2}$ (GeV)	Efficiency × BR (%)	Cross section (pb)	$\langle N \rangle$ (in 2 fb^{-1})
60	235	7.9 ± 1.1	0.16	25.2 ± 3.4
60	245	8.3 ± 1.1	0.08	12.8 ± 1.7
60	255	8.3 ± 1.1	0.06	10.5 ± 1.4
100	220	6.1 ± 0.8	0.10	12.2 ± 1.7
100	230	7.0 ± 1.0	0.08	11.3 ± 1.5
180	240	7.0 ± 0.9	0.05	7.1 ± 1.0
320	240	7.1 ± 0.9	0.05	6.9 ± 1.0

TABLE 6. Expected lower limits on the squark and gluino masses for the case of no SUSY detection at Run 2.

	Lower limit on $m_{\tilde{q}}$ (For any $m_{\tilde{g}}$)	Lower limit on $m_{\tilde{g}}$ (For any $m_{\tilde{q}}$)	Limit when $m_{\tilde{q}} = m_{\tilde{g}}$
Electrons			
Run 1	252 GeV	232 GeV	283 GeV
Run 2 (Scenario I)	430 GeV	490 GeV	490 GeV
Run 2 (Scenario II)	520 GeV	575 GeV	585 GeV
Muons			
Run 2	560 GeV	640 GeV	665 GeV

We assume that the neutralino (LSP) pairs are produced in cascade decays of other supersymmetric particles and use all SUSY pair production mechanisms when generating signal events.

Signal events were generated within the SUGRA framework with the following values of SUSY parameters: $A_0 = 0$, $\mu < 0$ and $\tan\beta = 2$ (the results are not sensitive to the value of A_0 .) Center of mass energy of the colliding beams was taken to be 2 TeV. ISAJET [53] was used for event generation. The acceptance and resolution of the DØ detector were parameterized using the following resolutions: $\delta E/E = 2\% \oplus 15\%/\sqrt{E}$ [GeV] (electrons), $\delta(1/p)/(1/p) = 0.018 \oplus 0.008(1/p)$ (muons), and $\delta E/E = 3\% \oplus 80\%/\sqrt{E}$ [GeV] (jets) and found consistent with the full detector simulation based on GEANT [69].

Figure 23 shows the points in the $(m_0, m_{1/2})$ SUGRA parameter space where signal Monte Carlo events were generated for the electron channel. Similar points were studied for the muon-decay channel.

C Selection criteria for the dielectron channel

A multijet trigger was used for the analysis of Run 1 data. It was found to be nearly 100% efficient for the typical RPV signal. Since the Run 2 trigger list will include a similar trigger, we assume trigger efficiency of 100% and do not perform any trigger simulations for the Run 2 analysis.

The following offline selections were used:

- At least two good electrons, the leading one with $E_T(e) > 15$ GeV and the other one with $E_T(e) > 10$ GeV;
- Rapidity range $|\eta| \leq 1.1$ (central calorimeter), or $1.5 \leq |\eta| \leq 2.5$ (end calorimeters) for all the electrons;
- Energy isolation for the electrons: the EM energy in the R=0.2 cone about the center of gravity of the EM cluster, subtracted from the total energy in R=0.4 cone, should not exceed 15% of the EM energy in the R-0.2 cone.
- At least four jets with $E_T(j) > 15$ GeV and $|\eta| < 2.5$;

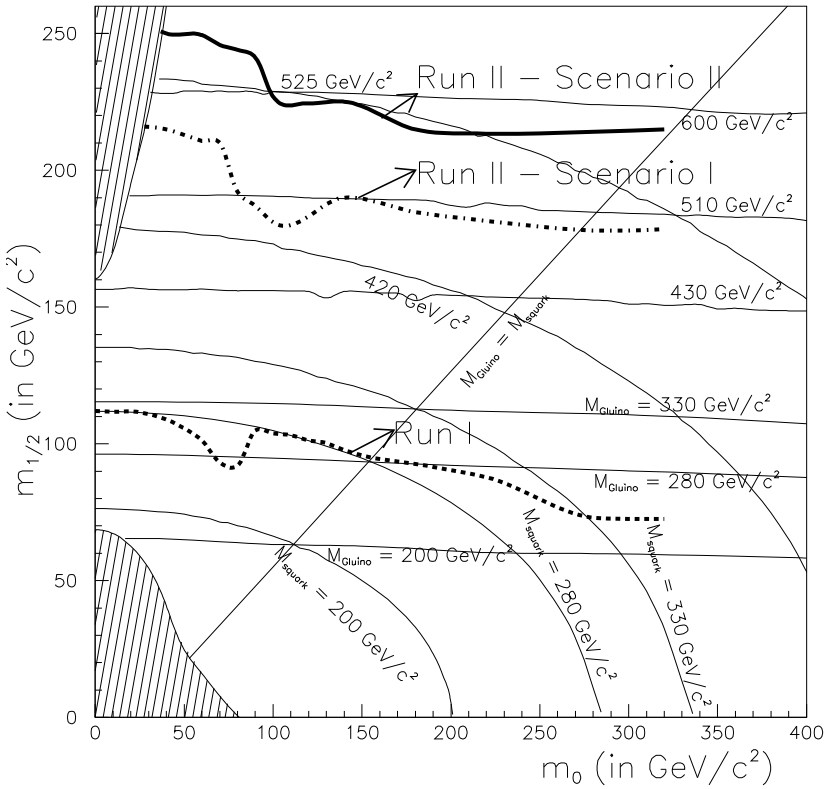

FIGURE 24. Estimated exclusion contour for Run 2 in the $(m_0, m_{1/2})$ plane for $tan\beta = 2$, $A_0 = 0$, $\mu < 0$, from the $ee + 4$ jets channel, assuming no SUSY signal is observed. Scenario I corresponds to a background of $36 \pm 4 \pm 6$ events (direct scaling from Run 1); scenario II uses the background of $15 \pm 1.5 \pm 1.5$ events (scaling, but with improvements in the detector taken into account).

- The dielectron invariant mass (M_{ee}) should not be in the Z-mass interval, ie, $\mid M_{ee} - M_Z \mid > 15$ GeV/c^2.

In the present analysis we have dropped the requirement on $H_T = \sum E_T(e) + \sum E_T(j)$, but retained all other offline criteria that were used in the previous analysis of data from Run I [26].

D Selection in the dimuon channel

The following event selection requirements were used for the muon decay channel:

- Two muons, the leading one with $p_T > 15$ GeV, and the other one with $p_T > 10$ GeV.
- Rapidity range $|\eta| < 2.3$ for both muons.
- Energy isolation requirement for both muons, i.e. the calorimeter energy accompanying the muon in a $(\eta\ \phi)$ cone of 0.4 should be consistent with that from a minimum ionising particle.
- At least four jets with $E_T(j) > 15$ GeV and $|\eta| < 2.5$;

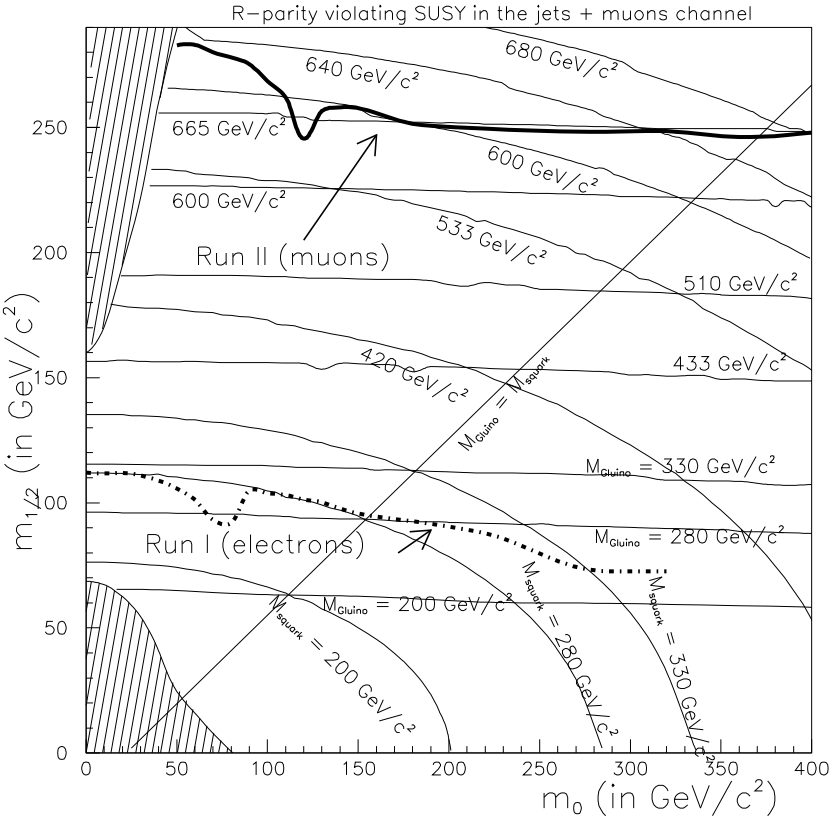

FIGURE 25. Estimated exclusion contour for Run 2 in the $(m_0, m_{1/2})$ plane for $tan\beta = 2$, $A_0 = 0$, $\mu < 0$, from the $\mu\mu + 4$ jets channel for background of $10 \pm 1.0 \pm 1.0$ (direct scaling from Run 1).

E Signal efficiencies

The number of signal events expected can be written as: $\langle N \rangle = \mathcal{L} \cdot \sigma \cdot \epsilon$, where $\langle N \rangle$ is the expected number of events for luminosity $\mathcal{L}$, σ is the cross-section, and ϵ is the overall efficiency. The efficiency ϵ can be split into three terms: $\epsilon = \epsilon_{\rm trig} \cdot \epsilon_{\rm kin} \cdot \epsilon_{\rm id}$. Here $\epsilon_{\rm trig}$ is the trigger efficiency for the events that pass the offline cuts (assumed to be 100%), $\epsilon_{\rm kin}$ is the efficiency for offline criteria, which includes kinematic, fiducial and topological requirements, and $\epsilon_{\rm id}$ is the electron/jet identification efficiency.

The efficiency for identifying jets is very high ($> 95\%$) and is expected to stay the same in Run 2.

Electron identification efficiencies in Run 1 were $80 \pm 7\%$ in the central ($|\eta| < 1.1$) and $71 \pm 7\%$ in the forward ($1.5 < |\eta| < 2.5$) regions [26]. These efficiencies were calculated for electrons with $E_T(e) > 25$ GeV, It drops by about 30% for electrons with $E_T(e) = 10$ GeV.

The muon identification efficiencies used in Run 1 were $62 \pm 2\%$ in the central ($|\eta| < 1.0$) and $24 \pm 4\%$ in the forward ($1.0 < |\eta| < 1.7$) regions [70]. These were calculated for muons with $p_T > 15$ GeV. For muons with 10 GeV $< p_T < 15$ GeV the efficiencies were 80% smaller on average [71].

In the present analysis we have taken the overall particle identification efficiency to be 0.90 ± 0.09 in each channel, independent of lepton E_T, primarily due to the expectation of a better tracker and muon spectrometer for the upgraded DØ experiment.

F Backgrounds

The main backgrounds are expected to arise from Drell-Yan production in association with four or more jets, dilepton top-quark events, and QCD multijet events. The latter is the dominant background for the electron channel (followed by the Drell-Yan background). In the case of muons, the background is dominated by the Drell-Yan and top pair production. We used Monte Carlo to calculate background from the first two sources, and data to estimate background from QCD jets.

Background for the Run 1 analysis was estimated to be $1.8 \pm 0.2 \pm 0.3$ (with 1.27 ± 0.24 from QCD and $0.42 \pm 0.15 \pm 0.16$ from the other processes) for $\sim 100\ pb^{-1}$ of data. To extrapolate this number to the data set from Run 2, we have simply multiplied it by the ratio of luminosities to obtain $36 \pm 4 \pm 6$ events. However, it is expected that due to the central magnetic field in the upgraded DØ detector, the probability of jets to be misidentified as electrons will be reduced by a factor of ~ 2 in Run 2. We have therefore considered a second scenario with the smaller expected background of $15 \pm 1.5 \pm 1.5$ events.

For the muon channel, the expected background has been scaled directly from the Run 1 analysis. We expect $10 \pm 1 \pm 1$ background events in Run 2.

G Results

In order to obtain the sensitivity of Run 2 in to RPV decays, we calculated the efficiency for signal for all the mass points shown in Fig. 23. Typical efficiencies, the signal cross section in the $ee + 4$ jets channel, and the expected event yield in 2 fb^{-1} of data, for several representative $(m_0, m_{1/2})$ points, are given in Table VII A. Similar numbers are obtained for the muon channel.

We use these efficiencies to obtain exclusion limits in the $(m_0, m_{1/2})$ plane at 95% CL, assuming that no excess of events will be observed above the predicted background. The exclusion contours for the electron and muon channel are shown in Fig. 24 and 25, respectively. Numerical values of the limits are summarized in Table VII A.

It's worth mentioning that our analysis provides a conservative estimate of the sensitivity achievable in Run 2, since no formal optimization of the signal vs. background has been performed. We expect that a formal optimization can improve the sensitivity in the mass reach by 15–20%.

VIII SPARTICLE PAIR PRODUCTION WITH BARYONIC DECAYS: DIFFICULT SCENARIOS FOR SUSY DETECTION AT THE TEVATRON

H. Baer, K. Cheung, J. Gunion

A Motivation

GUT scale boundary conditions (*e.g.* the mSUGRA universal boundary conditions) in which the gaugino soft-SUSY-breaking masses are assumed to have a common value at M_U lead to ratios of 7:2:1 (at low energy) for $m_{\widetilde{g}} : m_{\widetilde{\chi}_1^\pm} : m_{\widetilde{\chi}_1^0}$ due to $M_3 : M_2 : M_1 = \alpha_3 : \alpha_2 : \alpha_1$. In particular, the LSP $\widetilde{\chi}_1^0$ is bino-like and thus substantially lighter than the wino-like $\widetilde{\chi}_1^\pm$. However, there are well motivated models in which $M_1 > M_2$.

- In the context of string models, if the dilaton F component does not acquire a large vacuum expectation value (the most natural result in many models), then the leading contributions to gaugino masses will arise from loop corrections. This was first noted in the context of the the O-II model of Ref. [72] in the limit where supersymmetry breaking is ascribed entirely to the overall size modulus with none arising from the dilaton field. Including the possibility of a Green-Schwarz mixing term, parameterized by δ_{GS}, one has (at M_U):

$$M_3 : M_2 : M_1 \overset{O-II}{\sim} -(3 + \delta_{GS}) : (1 - \delta_{GS}) : (\frac{33}{5} - \delta_{GS})\,. \tag{18}$$

  At low energies, one finds $M_2 : M_1 = 2(1 - \delta_{GS}) : (33/5 - \delta_{GS})$. For δ_{GS} in the preferred range from 0 to -4, $M_2 < M_1$ and both the $\widetilde{\chi}_1^\pm$ and $\widetilde{\chi}_1^0$ are wino-like and very degenerate. More recently [73,74] the above

boundary conditions have been re-discovered (at least in the $\delta_{GS} = 0$ case) in a more general context. If the soft masses are dominated by the conformal anomaly, one obtains (to all orders in perturbation theory) $M_i = \frac{\beta_i(g_i^2)}{2g_i^2} m_{3/2}$. Going to low energy scales this translates into

$$M_1 = \frac{11\alpha}{4\pi \cos^2\theta_W} m_{3/2}\,, \quad M_2 = \frac{\alpha}{4\pi \sin^2\theta_W} m_{3/2}\,, \quad M_3 = -\frac{3\alpha_s}{4\pi} m_{3/2}\,, \tag{19}$$

as consistent with the evolved result of Eq. (18) when $\delta_{GS} = 0$.

- $M_2 < M_1$ at low energies can also arise if SUSY is broken by an F-term that is not an SU(5) singlet [75]. Recall that the M_a arise from a chiral superfield Φ that appears linearly in the gauge kinetic function with $\langle F\rangle \neq 0$ for its auxiliary component.

$$\mathcal{L} = \int d^2\theta W_a W_b \frac{\Phi_{ab}}{M_{\rm P}} + h.c. \sim \frac{\langle F_\Phi\rangle_{ab}}{M_{\rm P}} \lambda_a \lambda_b\,, \tag{20}$$

where $\lambda_{a,b}$ $(a,b = 1,2,3)$ are the gaugino fields. In the general case, $\Phi, F_\Phi \in (\mathbf{24}\times\mathbf{24})_{\rm symmetric} = \mathbf{1} \oplus \mathbf{24} \oplus \mathbf{75} \oplus \mathbf{200}$. Only F_Φ components that are 'neutral' under SU(3), SU(2), U(1) can have a vev if these groups are unbroken after SUSY breaking. As a result, $\langle F_\Phi\rangle_{ab} = c_a \delta_{ab}$, with c_a depending on the representation. c_a is independent of a for the $\mathbf{1}$ representation (universal M_a at M_U) but $M_2 < M_1$ for the $\mathbf{200}$ representation.

To give some specific results, at M_U (M_0) the O-II model with $\delta_{GS} = -4$ yields $M_3 : M_2 : M_1 = 1 : 5 : 53/5$ $(6 : 10 : 53/5)$ while the $\mathbf{200}$ model yields $1 : 2 : 10$ $(6 : 4 : 10)$. Even though M_2 is only slightly less than M_1 at low energies in the O-II and $\mathbf{200}$ models, $\Delta m_{\widetilde{\chi}} \equiv m_{\widetilde{\chi}_1^\pm} - m_{\widetilde{\chi}_1^0} <$ a few GeV is typical. Note that in both models $m_{\widetilde{g}}$ is close to the common $\widetilde{\chi}_1^\pm, \widetilde{\chi}_1^0$ mass.

The phenomenology for a model in which $M_2 < M_1$ and R-parity is conserved was explored in [76,77] (see also [78]). There it was noted that at an e^+e^- collider it will be virtually impossible to see $\widetilde{\chi}_1^+\widetilde{\chi}_1^-$ pair production since the potentially visible particles in $\widetilde{\chi}_1^\pm \to \widetilde{\chi}_1^0 + \ldots$ decays will be *very* soft. One can evade this problem by tagging the $\widetilde{\chi}_1^+\widetilde{\chi}_1^-$ event with a photon, *i.e.* look for $e^+e^- \to \gamma\widetilde{\chi}_1^+\widetilde{\chi}_1^-$. Sensitivity is substantially reduced compared to normal mSUGRA boundary conditions. At hadron colliders, if $m_{\widetilde{\chi}_1^\pm} \simeq m_{\widetilde{\chi}_1^0}$ one loses the tri-lepton signal from $\widetilde{\chi}_2^0\widetilde{\chi}_1^\pm \to \ell^+\ell^-\ell'^\pm + \not{p}_T$ since the $\ell'^\pm$ is too soft to be detected. Further, the like-sign di-lepton signal from $\widetilde{g}\widetilde{g}$ production (for instance) deriving from $\widetilde{g}\widetilde{g} \to 4j + \widetilde{\chi}_1^\pm\widetilde{\chi}_1^- \to 4j + \ell^\pm\ell'^\pm + \not{p}_T$ will also be undetectable. Still, as summarized in more detail later, in an R-parity conserving model the jets+$\not{p}_T$ signal will remain and allow reasonable (although somewhat reduced compared to mSUGRA) sensitivity to SUSY particle production [77].

B Baryon Number Violation

This leads us to the worst-case scenario in which we allow for baryonic R-parity violation. We consider the case where the leptonic R-parity violating terms are zero ($\lambda_{ijk}, \lambda'_{ijk}, \kappa_i = 0$) and only λ'' is non-zero. We note that λ''_{pnm} must be antisymmetric in the n, m family indices (due to the implicit antisymmetric colour coupling). For example, converting to a notation where p, n, m are given in terms of the quark type, we might imagine $\lambda''_{uds} = -\lambda''_{usd} \neq 0$.

The most obvious implication of baryonic R-parity violation is the possible absence of any specifically supersymmetric source of missing energy. The decay products of the $\widetilde{\chi}_1^0$-LSP[3] would be jets that would be visible in the detector provided the decays are prompt. Combining baryonic R-parity violation with $\widetilde{\chi}_1^\pm - \widetilde{\chi}_1^0$ degeneracy provides some very unusual and, in some cases, very difficult scenarios for detecting supersymmetry.

Of course, there are various means for placing bounds on some of the λ''_{ijk} (see, *e.g.* , [79] and [2]). Perturbativity up to the GUT scale requires that all λ'''s be < 1. The experimental limit on the $\Delta B = \Delta S = -2$ decay $^{16}O \to {}^{14}C + K^+ + K^+$ [14,80] leads to $|\lambda''_{usd}| < 5.6 \times 10^{-7} \left(\frac{200\ \rm MeV}{\tilde{\Lambda}_{QCD}}\right)^{5/2} \left(\frac{m_{\tilde{g}}}{100\,GeV}\right)^{1/2} \left(\frac{m_{\tilde{q}}}{1\ \rm TeV}\right)^2$. Here,

[3] We do not have space here to consider the $\widetilde{g}$-LSP case that is also possible for O-II model boundary conditions when $\delta_{GS} \sim -3$.

$\widetilde{\Lambda}_{QCD}$ is a scale that dimensional analysis suggests should be of order $\Lambda_{QCD} \sim 200$ MeV. Constraints on λ''_{ubd}, λ''_{tsd} and λ''_{tbd} from $N \longrightarrow \overline{N}$ oscillation limits (see Ref. [79]) vary roughly as $1/M^4_{L-R}$, where M^2_{L-R} is the $L-R$ mixing entry in the relevant squark mass-squared matrix. We assume that $L-R$ mixing can be neglected, implying that M^2_{L-R} is small and that these bounds are not relevant. $2 \to 2$ processes such as $u + d \to \widetilde{d}^* \to \overline{d}\widetilde{\chi}^0_1$ disturb the standard baryogenesis picture *if sphalerons are present* and if any $|\lambda''|$ were larger than $\sim 5 \times 10^{-7}(m_{\widetilde{q}}/1\text{ TeV})^{1/2}$, a very severe constraint. However, these constraints do not apply if sphalerons are not present at the appropriate epoch [8]. Bounds that can be placed on various products of the λ'''s are not relevant to our analysis since we shall consider only one coupling to be non-zero at a time.

C Phenomenology

$\underline{\widetilde{\chi}^0_1 \text{ decays}}$

The expected $c\tau$ for the $\widetilde{\chi}^0_1$ is of considerable importance. If the $\widetilde{\chi}^0_1 \to u_R d_R d'_R$ (family indices implied) decay is prompt, discovering supersymmetry at a hadronic collider in this model is far from easy. However, if this decay has a significant path length, our ability to search for supersymmetry would be greatly enhanced by virtue of being able to look for a decay vertex. In the limit of a very long path length, we would revert to the jets+$\not{p}_T$ signature. This was studied in Refs. [76,77] for the present class of models. Since $m_{\widetilde{\chi}^\pm_1} \simeq m_{\widetilde{\chi}^0_1}$ and $m_{\widetilde{g}}$ is not that much larger than $m_{\widetilde{\chi}^\pm_1}$ supersymmetry signals are weaker than for mSUGRA boundary conditions. Still, the LHC would be guaranteed to find a signal for $m_{\widetilde{g}} \lesssim 1$ TeV; but at the Tevatron the weaker signals would imply a fairly limited discovery reach.

A result for the path length is easily given in the limit where the sfermions are much heavier than the $\widetilde{\chi}^0_1$. Assuming also that the relevant u-type and d-type squarks are more or less degenerate with mass $\widetilde{m}$ and neglecting $L-R$ squark mixing, one obtains

$$c\tau = .03\ \mu\text{m} \left(\frac{0.1}{N_{11}}\right)^2 \left(\frac{1}{\lambda''}\right)^2 \left(\frac{100\,GeV}{m_{\widetilde{\chi}^0_1}}\right)^5 \left(\frac{\widetilde{m}}{1\text{ TeV}}\right)^4 \left[1 - \frac{4}{5}\left(\frac{m^2_{\widetilde{\chi}^0_1}}{\widetilde{m}^2}\right) + \ldots\right], \tag{21}$$

where N_{ij} are the neutralino mixing matrix entries with i refering to $\widetilde{\chi}^0_{i=1,2,3,4}$ and j refering to B, W_3, H^0_1, H^0_2. Eq. (21) neglects the tiny contributions from the Higgsino components of $\widetilde{\chi}^0_1$. In the absence of $L-R$ squark mixing there is no contribution to the RPV decay of the $\widetilde{\chi}^0_1$ coming from its primary wino component (of size N_{12}). (This is because the RPV λ'' superpotential term only involves right-handed superfields.) In the model class being considered, $N_{11} \sim 0.1$ is typical and $\widetilde{m} > 1$ TeV is preferred (although this could be avoided in a 'no-scale' type model). For $\widetilde{m} \sim 1$ TeV, $\lambda'' < 0.017$ (< 0.0043) is required for $c\tau > 100$ μm if $m_{\widetilde{\chi}^0_1} \sim 100\,GeV$ ($\sim m_t$), respectively. For $\widetilde{m} \sim 300\,GeV$, the corresponding λ'' values must be smaller by a factor of .09 for $c\tau > 100$ μm. Given that typical Yukawa couplings for the heavier 'light' quarks are $gm_s/(2m_W) \sim 0.0008$ and $gm_c/(2m_W) \sim 0.006$, the RPV analogues could easily be this small.

For the constraint given earlier on λ''_{usd}, the $\widetilde{\chi}^0_1$ would have a very long path length if all other λ'''s are zero. However, it seems likely that the higher generation λ'''s would be larger than λ''_{usd}. The largest λ'''s might be those associated with the 3rd family. However, since the mass of the $\widetilde{\chi}^0_1$ is typically not very large in the models we consider, a top quark in the final state might have to be virtual, implying substantial phase-space suppression. The values for $c\tau \times [|\lambda''|^2 |N_{11}|^2]$ for $t^{(*)}bd$, $t^{(*)}bs$ and $t^{(*)}sd$ are plotted in Fig. 26 in comparison to that obtained in any one of the *usd*, *ubd*, *ubs*, *csd*, *cbd* and *cbs* channels. At $m_{\widetilde{\chi}^0_1} = 100\,GeV$ ($175\,GeV$), one of the three virtual top channels would dominate over one of the other six channels if λ'' for the former is a factor of $\sim 5 \times 10^4$ (~ 500) larger than for the latter. Keeping in mind that Yukawa couplings differ by ratios of $\sim m_t/m_u \sim 5 \times 10^4$ and $\sim m_t/m_s \sim 350$, such large ratios should not be regarded as impossible.

Typical $c\tau$ values for the various decays are obtained from Fig. 26 by multiplying by $1/|N_{11}|^2 \sim 100$ and by $1/|\lambda''|^2$. If $\widetilde{\chi}^0_1$ decay is dominated by a virtual top channel and the relevant $\lambda'' \sim 1$, a path length of order 100 m (100 μm) is to be expected for $m_{\widetilde{\chi}^0_1} \sim 100\,GeV$ ($\sim m_t$). For smaller λ'', $c\tau$ is even larger. However, if one of the $\lambda_{usd,\ldots}$ is substantial, the $\widetilde{\chi}^0_1$ decay will be very prompt.

$\underline{\widetilde{\chi}^\pm_1 \text{ decays}}$

In the models being considered, $\Delta m_{\widetilde{\chi}} \equiv m_{\widetilde{\chi}^\pm_1} - m_{\widetilde{\chi}^0_1} < 1\,GeV$ is typical and the $c\tau$ for $\widetilde{\chi}^\pm_1 \to \widetilde{\chi}^0_1 \ldots$ (see [78]) can be so large that the $c\tau$ for direct RPV decay of the $\widetilde{\chi}^\pm_1$ (values being comparable to those plotted for

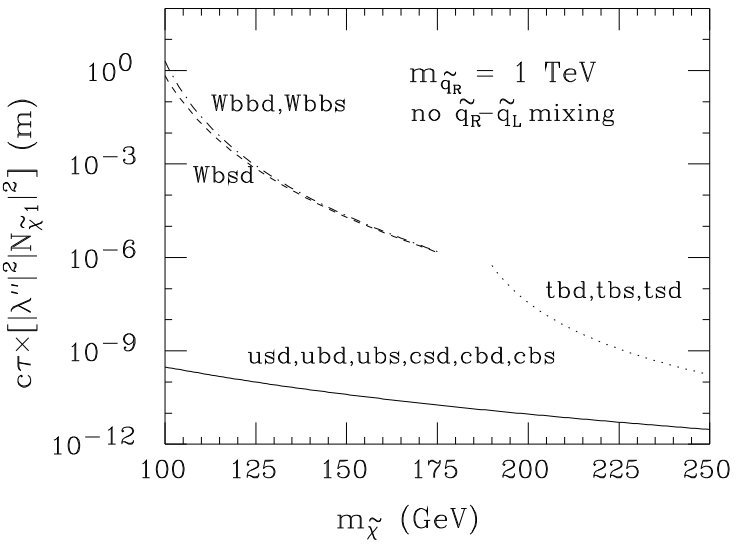

FIGURE 26. We plot $c\tau \times [|\lambda''|^2|N_{11}|^2]$ as a function of $m_{\widetilde{\chi}_1^0}$ for a variety of final states, including those arising from virtual top intermediate states.

the $\widetilde{\chi}_1^0$) can easily be shorter (*i.e.* the width larger). In such scenarios, direct $\widetilde{\chi}_1^\pm$ decays to the $\widetilde{\chi}_1^0$ might be quite rare. Phenomenologically, however, it would hardly make a difference since the decay products of the $\widetilde{\chi}_1^\pm$ decay are so soft for the small expected values of $\Delta m_{\tilde{\chi}}$ anyway.

$\underline{\widetilde{\boldsymbol{g}} \text{ decays}}$

The normal SUSY $\widetilde{g} \to q\overline{q}\widetilde{\chi}_1^0$ amd $\widetilde{g} \to q'\overline{q}\widetilde{\chi}_1^\pm$ decays compete with the RPV $\widetilde{g} \to \overline{q}\overline{q}\widetilde{q}_R^* \to 3\overline{q}$ decays. For our boundary conditions, the former SUSY modes can be sufficiently phase space suppressed that the RPV decays could dominate if one or more of λ''_{usd}, λ''_{ubd}, λ''_{ubs}, λ''_{csd}, λ''_{cbd}, or λ''_{cbs} were large. However, this would result in little change in the phenomenology since the extra 2 jets coming from the SUSY $\widetilde{g}$ chain decays would generally be quite soft and not easily reconstructed at a hadron collider. At an e^+e^- collider, $\widetilde{g}$ production (via $e^+e^- \to q\overline{q}\widetilde{g}\widetilde{g}$) has a small cross section and $\widetilde{g}$ decays are not an important issue.

D SUSY detection at a hadron collider

Various possible scenarios could emerge. Suppose first that the relevant λ'' is sufficiently small that the $\widetilde{\chi}_1^0$ is effectively stable in the detector. Then, the R-parity conserving results of Ref. [77] for $m_{\widetilde{g}} \sim m_{\widetilde{\chi}_1^\pm} \simeq m_{\widetilde{\chi}_1^0}$ apply. Since the lepton from $\widetilde{\chi}_1^\pm \to \ell^\pm\widetilde{\chi}_1^0$ decay is very soft, standard SUSY signals relying on leptons are no longer viable. This includes the like-sign dilepton signal for $\widetilde{g}\widetilde{g}$ production in which $\widetilde{g}\widetilde{g} \to 4j + \widetilde{\chi}_1^+\widetilde{\chi}_1^+ + X \to 4j + \ell^+\ell^+ + \not{E}_T$ (or the charge conjugate) and the trilepton signal from $\widetilde{\chi}_1^\pm\widetilde{\chi}_2^0 \to \ell^\pm\ell'^+\ell'^-$. One must rely entirely on the jets plus missing energy signal for $\widetilde{g}\widetilde{g}$ production, which is weakened by the fact that the jets in both $\widetilde{g} \to q'\overline{q}\widetilde{\chi}_1^\pm$ and $\widetilde{\chi}_1^\pm \to q'\overline{q}\widetilde{\chi}_1^0$ decays are no longer hard enough to pass typical cuts used by CDF and D0 to define a visible jet. The only energetic high-p_T jets present are those arising from initial state radiation. Due to the smaller number of jets passing cuts, discovery reach at the Tevatron is substantially reduced compared to the normal mSUGRA scenario, even if the relatively soft (as appropriate for the scenario being considered) Run I CDF and D0 cuts are employed. This is illustrated in Table 7.

Next, suppose λ'' is of 'moderate' magnitude such that $\widetilde{\chi}_1^0$ decay is visible in the detector, *i.e.* has a path length leading to a visible vertex in the inner vertex detector or tracker or a recognizable delayed decay in the outer portions of the detector. The combined requirement of many jets and a clear vertex or delayed decay should leave very little QCD background. Supersymmetry discovery would be largely limited by event rate and discovery reach would exceed even that typical of mSUGRA boundary conditions.

The most difficult case for supersymmetry discovery would be that in which λ'' is sufficently large that the RPV $\widetilde{\chi}_1^0$ decay is prompt and the λ'''s involving the top/stop are sufficiently small that the virtual or real top-quark decay modes of the $\widetilde{\chi}_1^0$ are not important and we must consider $\widetilde{\chi}_1^0 \to 3j$ decays. In this case,

TABLE 7. Maximum $m_{\widetilde{g}}$ values that can be probed using D0 and CDF Run I cuts in the $jets + \not\!\!E_T$ final state for different integrated luminosities, L, at the Tevatron and Tev33 using the O-II model boundary conditions with $\delta_{GS} = -4.5$. Observability is defined by $S/\sqrt{B} \geq 5$ and $S/B \geq 0.2$. Also given are the maximum $m_{\widetilde{g}}$ values for which $\widetilde{g}\widetilde{g}$ production can be observed in the case of mSUGRA universal boundary conditions for both Run I cuts and also stronger cuts optimized for Run II/TeV33. The results of this table are for $\tan\beta = 2$ and $\mu < 0$.

Cuts	$L =$	8 pb^{-1}	19 pb^{-1}	100 pb^{-1}	2 fb^{-1}	25 fb^{-1}
D0	$\delta_{GS} = -4.5$	—	$80\,GeV$	$110\,GeV$	$150\,GeV$	$150\,GeV$
RunI	mSUGRA	—	$140\,GeV$	$200\,GeV$	$200\,GeV$	$200\,GeV$
CDF	$\delta_{GS} = -4.5$	$100\,GeV$	$130\,GeV$	$140\,GeV$	$160\,GeV$	$160\,GeV$
RunI	mSUGRA	$150\,GeV$	$170\,GeV$	$210\,GeV$	$240\,GeV$	$240\,GeV$
Strong	mSUGRA	$m_{\widetilde{g}}$ excluded by $m_{\widetilde{\chi}_1^\pm} \leq 47\,GeV$			$250\,GeV$	$300\,GeV$

$3j = uds$, udb, usb, cds, cdb, and/or csb are all, in principle, possible. There would be no specifically SUSY source of missing energy in sparticle-pair production. The most characteristic feature of $\widetilde{g}\widetilde{g}$ production would be the presence of many energetic jets in most events. To explore the characteristics of such events in more detail, we have considered a sample case defined by the following O-II (GUT scale) model parameters:

$$\delta_{GS} = -4.1, \quad m_0 = 1800\,GeV, \quad m_{1/2} = 10\,GeV, \quad A_0 = 0, \quad \tan\beta = 3, \quad \mu > 0\,, \tag{22}$$

leading to

$$\begin{aligned} &m_{\widetilde{g}} \sim 102\,GeV, \quad m_{\widetilde{\chi}_1^0} \simeq m_{\widetilde{\chi}_1^\pm} \sim 100\,GeV, \quad \Delta m_{\widetilde{\chi}} \sim 0.23\,GeV, \quad m_{\widetilde{\chi}_2^0} \sim 120\,GeV, \\ &m_{\widetilde{\chi}_2^\pm} \sim m_{\widetilde{\chi}_3^0} \sim m_{\widetilde{\chi}_4^0} \sim 1140\,GeV, \quad m_{\widetilde{\ell},\widetilde{q}} \sim 1.4 - 1.8 \text{ TeV}. \end{aligned} \tag{23}$$

Note the very low mass scales for all gauginos, including the $\widetilde{g}$, and the high mass scales (typical for the O-II boundary conditions) of all sfermions and higgsinos.

We have performed a Monte Carlo simulation of signal and background (using ISAJET [53]). We define jets using $E_T > 15\,GeV$, $|\eta| < 4$, and a cone size of $\Delta R = 0.5$. In Fig. 27(a), we plot the event rate for the QCD background as compared to that for supersymmetric particle pair production (all channels included, but mainly $\widetilde{g}\widetilde{g}$) as a function of the number of jets, n_j, before any tagging requirement, and before any other cuts. The signal has larger n_j on average, but the QCD background is still bigger by a factor of 10 even if we require $n_j \geq 8$. Nonetheless, if we compute the nominal $S/\sqrt{B}$ for the $n_j = 8$ bin, assuming $L = 2$ fb^{-1} (30 fb^{-1}), we get $S/\sqrt{B} = 45$ (170). Thus, if the systematic uncertainty for the $n_j = 8$ background could be reduced to below 10% we would achieve an observable signal without tagging. This might be possible by normalizing using the $n_j \leq 7$ bins once a reliable calculation of relative rates for multi-jet events with n_j ranging from low values up to $n_j = 8$ becomes available. (The ISAJET shower model results for relative rates are probably not accurate at the 10% level.)

However, the very strong limit on λ''_{usd} means that one (or more) of the ubd, ubs, csd, cbd, cbs channels will dominate $\widetilde{\chi}_1^0$ decay. All of these contain at least one heavy quark. Since SUSY pair production events contain at least two $\widetilde{\chi}_1^0$'s, we can then use double-tagging to reduce the background relative to the signal. For all but the cds decay channel, at least two of the jets in the final state will be b-jets. If cds decays dominate, we would have two c-jets. Since c-tagging will have lower efficiency than b-tagging, dominance of $\widetilde{\chi}_1^0$ decays by the cds channel results in the most difficult scenario for supersymmetry detection.

To explore this 'worst case', we assume $\widetilde{\chi}_1^0 \to csd$ exclusively. Fig. 27(b) gives the n_j distributions for signal and background after requiring that every accepted event contain at least two tagged jets. For this plot we use the CDF 'JP'-tag algorithm (designed for c quark tagging). We require that a tagged jet have $|\eta| < 2$ [4] and $p_T > 25\,GeV$. For such a jet, the JP-tag yields [81]: $\epsilon_b \geq 0.5\,, \quad \epsilon_c \geq 0.3\,, \quad$ for $\epsilon_{q,g} \sim 0.05\,,$ where $q = u, d, s$. [5] From Fig. 27(b), we see that after tagging it is best to focus on the $n_j = 7$ bin, with

[4] This is the rapidity coverage for Run II.

[5] For $p_T \geq 50\,GeV$, $\epsilon_b \sim 0.6$ and $\epsilon_c \sim 0.35$ for $\epsilon_{q,g} \sim 0.05$. If the L00 inner layer is constructed, ϵ_b (ϵ_c) will be larger by a factor of 1.12 (1.25).

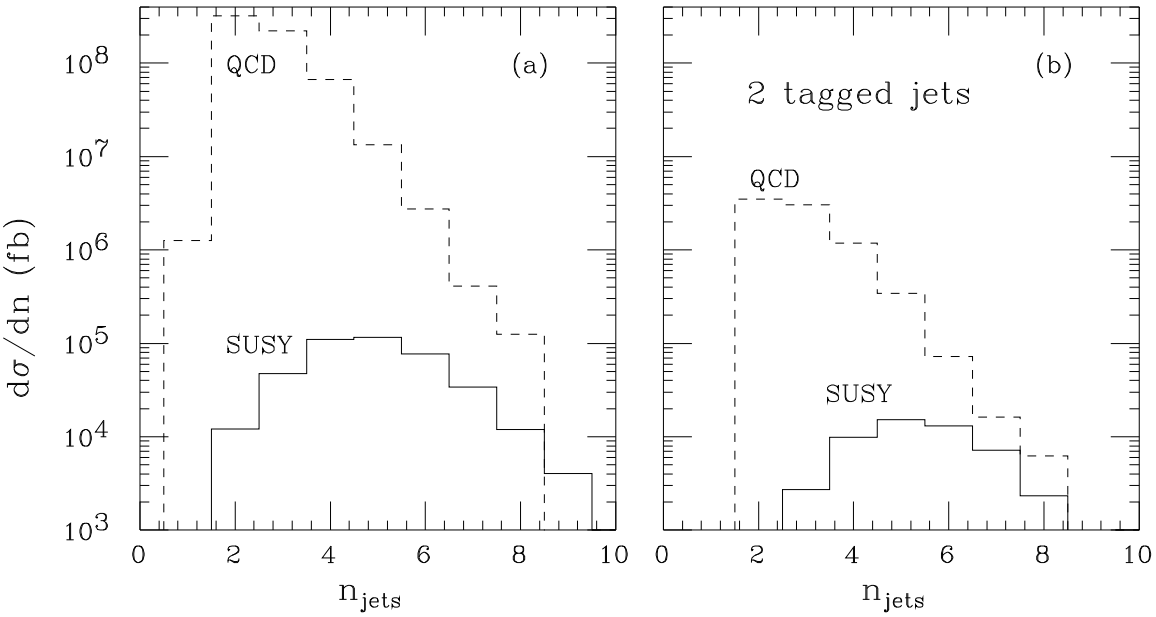

FIGURE 27. The number of events is plotted as a function of the number of jets for the QCD background (dashes) and for SUSY production processes (solid) (a) without tagging (b) after requiring that at least two jets be tagged (using the CDF JP charm tagging algorithm). O-II model parameters as in Eq. (22).

$S = 1.4\times10^4, B = 3.2\times10^4$ ($S = 2.1\times10^5, B = 4.8\times10^5$) for $L = 2$ fb^{-1} ($L = 30$ fb^{-1}), leading to $S/\sqrt{B} = 78$ ($S/\sqrt{B} = 303$) with $S/B \sim 45\%$ (a big improvement). Thus, for low-mass SUSY scenarios [see Eq. (23)] of the type being considered, double-tagging leads to a very clear excess (beyond Standard Model expectations) of events with a large number of jets.

At the low $m_{\widetilde{g}}$ value considered above, additional cuts in the variables $E_T^{\rm tot} \equiv \sum_j |E_T^j|$ and $H_T \equiv \sum_j |E_T^j| + \not\!\!E_T$ are not particularly helpful. However, in order to reduce the QCD background when searching for gluinos of substantially higher mass, cuts requiring high values for one or both of these variables are essential. For an appropriate cut, we would again examine the n_j distribution after requiring two tagged jets. We anticipate that a signal will be observable so long as the basic production rate for $\widetilde{g}\widetilde{g}$ pairs is substantial. The exact mass reach (in $m_{\widetilde{g}}$) is under study [82].

E Discussion and Conclusions

We have shown that observation of a signal from $\widetilde{g}\widetilde{g}$ pair production is likely to be possible at the Tevatron even in the extreme of O-II model boundary conditions and RPV $3j$ decays of the $\widetilde{\chi}_1^0$, so long as the gluino mass is not too large. However, the high-jet-number signal upon which we focused does not allow us to determine the strength of the dominant RPV λ'' coupling. There are two possibilities for directly determining λ''. If λ'' is large, RPV-induced single squark production cross sections are also typically substantial, and, if a signal can be isolated [82], the cross section size gives a measure of λ''. If λ'' is small, the decay path length for the $\widetilde{\chi}_1^0$ might be observable and would again provide a measure of λ''. However, our preliminary estimates [82] indicate that there is a region of intermediate λ'' at higher $m_{\widetilde{q}_R}$ for which neither $c\tau(\widetilde{\chi}_1^0)$ nor $\sigma(\widetilde{q}_R)$ will be measurable. In this region, determination of λ'' would only be possible if an RPV decay mode of the $\widetilde{\chi}_1^\pm$ is competitive with its standard SUSY decay modes and these can be separated from one another (which is not at all certain); the relative size of the branching ratios would then provide a measure of λ''. Parenthetically, we note that at an e^+e^- collider the only means for measuring λ'' would be via the $\widetilde{\chi}_1^0$ decay length; there are no sources of quarks or antiquarks as needed for squark production via baryonic RPV couplings.

To summarize, even if there is baryonic R-parity violation, implying absence of missing energy in SUSY events, the very large number of jets expected for a typical SUSY event will allow us to isolate the SUSY signal

so long as gluino (and/or squark) masses are sufficiently low that SUSY event rates are substantial. Further, there is at least a decent chance that we will be able to measure the strength of the RPV coupling.

Acknowledgments

This work was supported by the Department of Energy and by the Davis Institute for High Energy Physics.

PART 3: Spontaneous R-Parity Breaking

IX DECAYS OF THE TOP-QUARK AND THE TOP-SQUARK

F. de Campos, M.A. Díaz, O. J. P. Eboli, M. B. Magro, L. Navarro, W. Porod, D. A. Restrepo, and J.W.F. Valle

A Introduction

In this section we study the case of spontaneous R-parity breaking. This is a modification of the previous studies in that an extra superfields is added: ν_R, which is a gauge singlet and corresponds to a right-handed neutrino. Here we focus on the case of bilinear R–Parity Violation (BRPV) [83–86], where λ, λ', $\lambda'' = 0$ in Eq.(3) and $\kappa_i \neq 0$[6]. This includes as an additional feature a vev for the sneutrinos. These models are well-motivated theoretically as they arise as effective truncations of models where R–Parity is broken spontaneously [87] through *right handed* sneutrino vacuum expectation values (vev) $\langle \tilde{\nu}^c \rangle = v_R \neq 0$. They open new possibilities for the study of the unification of the Yukawa couplings [88]. In particular it has been shown that in BRPV models bottom-tau unification may be achieved at any value of $\tan\beta$. From a phenomenological point of view these models predict a plethora of novel processes [89] that could reveal the existence of SUSY in a totally different way, not only through the usual missing momentum signature as predicted by the MSSM. They provide a very predictive approach to the violation of R–Parity, which renders the systematic study of R-parity violating physics [89] possible.

We consider the simplest superpotential which violates R-Parity

$$W_{\not R_p} = W_{MSSM} + \epsilon_i \widehat{L}_i \widehat{H}_u \,, \tag{24}$$

assuming that TRPV terms are absent or suppressed, as would be the case if their origin is gravitational [90]. The ϵ_i terms violate lepton number in the ith generation, respectively. Models where R–Parity is broken spontaneously [87] through a vev of the right handed sneutrinos $\langle \tilde{\nu}^c \rangle = v_R \neq 0$ generate only BRPV terms. The ϵ_i parameters are then identified as a product of a Yukawa coupling and v_R. This provides the main theoretical motivation for introducing explicitly BRPV in the MSSM superpotential. For simplicity we set from now on $\epsilon_1 = \epsilon_2 = 0$. Thus we have tau–lepton signatures and we only test the case where tau–lepton number is violated. The MSSM–BRPV has the following superpotential

$$W_{\not R_p} = \varepsilon_{ab} \left[h_t \widehat{Q}_3^a \widehat{U}_3 \widehat{H}_u^b + h_b \widehat{Q}_3^b \widehat{D}_3 \widehat{H}_d^a + h_\tau \widehat{L}_3^b \widehat{R}_3 \widehat{H}_d^a + \mu \widehat{H}_u^a \widehat{H}_d^b + \epsilon_3 \widehat{L}_3^a \widehat{H}_u^b \right] \,, \tag{25}$$

where the first four terms correspond to the MSSM. The last term violates tau–lepton number as well as R–Parity.

In this model the top-quark and the top-squark get additional decay modes, e.g. $t \to \tilde{\tau}_1^+ \, b$ or $\tilde{t}_1 \to \tau^+ + b$. We study these decays in view of the Tevatron (for top decays in TRPV models see [91]). We show that existing Tevatron data give additional constraints on the parameter space and extrapolate to Run II.

B Top Decays

One of the major successes of the Tevatron has been the discovery of the top-quark [92]. The large top mass implies a relatively small production cross section at the Tevatron. Therefore, the sum of all branching ratios of the top decays except $t \to W^+ \, b$ is only restricted to be smaller than approximately 25 % [93]. In the MSSM

[6] Throughout the rest of this section we shall denot the parameter κ as ϵ.

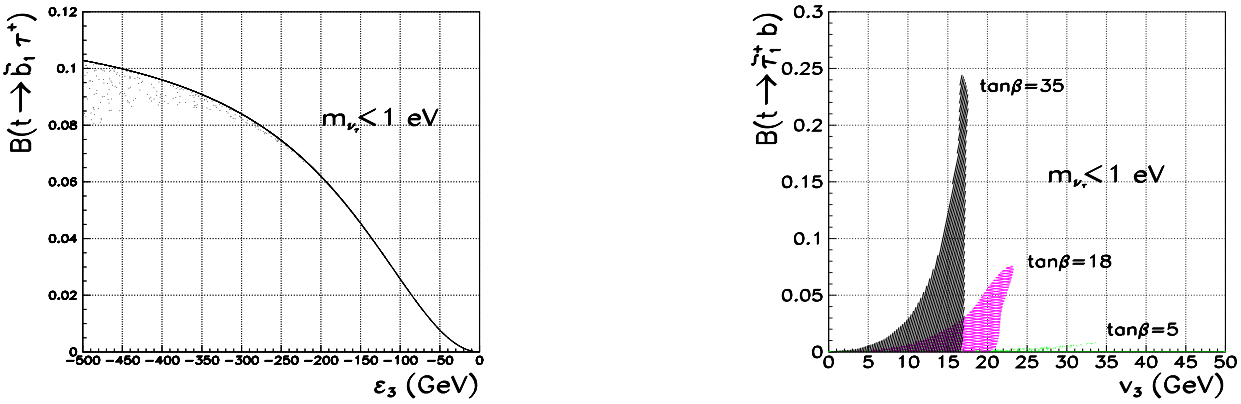

FIGURE 28. (a) Branching Ratios for $t \to \tilde{b}_1\,\tau^+$ as a function of ϵ_3. (b) Branching Ratios for $t \to \tilde{\tau}_1^+\,b$ as a function of v_3 for different values of $\tan\beta$. In both cases the parameters are: $M = 180$ GeV, $\mu = 200$ GeV, $\tan\beta = 35$, $M_{E_3} = 285$ GeV, $A_\tau = 280$ GeV, $M_Q = 285$ GeV, $M_U = 180$ GeV, $M_D = 190$ GeV, $A_t = 320$ GeV, $A_b = 120$ GeV, $B = 50$ GeV, -500 GeV $< \epsilon < 0$ GeV, 0 GeV $< B_2 <$ 200 GeV, 1 GeV $< v_3 <$ 50 GeV.

the top can decay according to: $t \to W^+\,b$, $t \to H^+\,b$, $t \to \tilde{\chi}_1^0\,\tilde{t}_1$, $t \to \tilde{\chi}_1^+$. [7] In the BRPV model the charginos mix with the charged leptons, the neutralinos with neutrinos, and the charged sleptons with the charged Higgs boson [83–85]. Therefore, the top can have additional decay modes:

$$t \to \tilde{\tau}_1^+\,b\,, \quad t \to \nu_\tau\,\tilde{t}_1\,, \quad t \to \tau^+\,\tilde{b}_1\,. \tag{26}$$

As an illustrative example, we show in Fig. 28a the branching ratio for $t \to \tau^+\,\tilde{b}_1$ as a function of a) ϵ_3 and b) v_3. We have randomly chosen 10,000 points imposing the following experimental constraints: $m_{\nu_\tau} < 18$ MeV, $m_{\tilde{t}_1}, m_{\tilde{b}_1} > 80$ GeV, $min(m_{H^+}, m_{\tilde{\tau}_1}) > 70$ GeV, and $m_{\tilde{\chi}_1^+} > 85$ GeV. The parameters are listed in the figure caption. We find a strong correlation between the R-parity decay branching ratio $BR(t \to \tau^+\,\tilde{b}_1)$ and the magnitude of ϵ_3. This can be understood in the following way: in the chargino mass matrix the mixing between the leptons and the charginos disappears if one does the following rotation in the superfields: $\widehat{H}_1 \to N(\mu\widehat{H}_1 - \epsilon_3\widehat{L}_3)$ and $\widehat{L}_3 \to N(\mu\widehat{L}_3 + \epsilon_3\widehat{H}_1)$ (N being the normalization). In this basis the coupling between t, τ, and $\tilde{b}_1$ is proportional $N\,h_b\,\epsilon_3$ leading to this feature.

In Fig. 28b we show the branching ratio for $t \to \tilde{\tau}_1^+\,b$ as a function of v_3. As in Fig. 28a, results in Fig. 28b are displayed for different values of $\tan\beta$ and the other parameters are also the same. The dependence on $\tan\beta$ is a result of: (i) The stau - charged Higgs boson mixing is proportional to the R-parity breaking parameters ϵ_3 and v_3 (ii) The decay width depends on the bottom Yukawa coupling which increases with $\tan\beta$. As can be seen from the figure, there is a strong correlation between the magnitude of the R-parity breaking branching ratios and the mixing between the stau and the charged Higgs boson.

We have performed a similar scan for small $\tan\beta$ for both of BRPV decay channels discussed above. These are suppressed in this case and can not exceed 2% or so, i.e. $\sum BR(t \to b\,X) < 1 - 2\%\,(X \neq W)$), because their decay widths are in all cases proportional to the bottom Yukawa coupling squared. In the case of $t \to \tau^+\,\tilde{b}_1$ this is clear from the discussion of Fig. 28a. In the case of $t \to \tilde{\tau}_1^+\,b$ one has to note that the stau mixes mainly with the charged component of the down-type Higgs multiplet H_1 ($\tilde{\tau}_L$ and H_1 have the same gauge quantum numbers) and the $H_1 tb$ coupling is proportional to h_b.

In every case the various decay modes lead to the cascade decays

$$t \to \tilde{\tau}_1^+\,b \to \left\{ \begin{array}{ll} \tau^+\,\nu_\tau\,b & \\ \tau^+\,\tilde{\chi}_1^0\,b & \to \left\{ \begin{array}{l} \tau^+\,f\,\bar{f}\,\nu_\tau\,b \\ \tau^+\,f\,\bar{f}'\,\tau^\pm\,b \end{array} \right. \\ \nu_\tau\,\tilde{\chi}_1^+\,b & \to \left\{ \begin{array}{l} \nu_\tau\,f\,\bar{f}'\,\nu_\tau\,b \\ \nu_\tau\,f\,\bar{f}\,\tau^+\,b \end{array} \right. \\ c\,s\,b & \end{array} \right. \quad , \qquad t \to \tau^+\,\tilde{b}_1 \to \left\{ \begin{array}{l} \tau^+\,\nu_\tau\,b \\ \tau^+\,\tilde{\chi}_1^0\,b \to \left\{ \begin{array}{l} \tau^+\,f\,\bar{f}\,\nu_\tau\,b \\ \tau^+\,f\,\bar{f}'\,\tau^\pm\,b \end{array} \right. \end{array} \right. \tag{27}$$

[7] The mode $\tilde{b}_1$ is practically ruled out by existing LEP2–data [94].

In nearly all cases there are two τ's and two b-quarks in the final state plus the possibility of additional leptons and/or jets. Therefore, b-tagging and a good τ identification are important for extracting these final states. Moreover there is in general a large multiplicity of charged particles in the final state which should be helpful in reducing the background. The background will come mainly from the production of one or two gauge bosons plus additional jets. The conclusion in similar cases [95] has been that in its next run the Tevatron should be sensitive to branching ratio values up to $10^{-3} - 10^{-2}$ depending on the mode. Therefore, the possible observation of one of these additional decay modes at the Run II of the Tevatron should give a strong hint on the underlying parameters.

C Top-Squark Decays

Top-squark physics is a very interesting part of supersymmetric theories, because the lighter top-squark might be the lightest charged SUSY particle [58]. In the kinematic region accessible to the Tevatron the light top-squark has the following MSSM decay modes: $\tilde{t}_1 \to \tilde{\chi}_i^+ + b$, $\tilde{t}_1 \to \tilde{\chi}_1^0 + c$, $\tilde{t}_1 \to \tilde{l}_i^+ + \nu_l + b$, $\tilde{t}_1 \to \tilde{\nu}_l + l^+ + b$, $\tilde{t}_1 \to \tilde{\chi}_1^0 + W^+ + b$, and $\tilde{t}_1 \to \tilde{\chi}_1^0 + H^+ + b$ (for a discussion see e.g. [96] and references therein). In BRPV models the top-squark has an additional and phenomenologically very interesting decay mode [97]:

$$\tilde{t}_1 \to \tau^+ + b \tag{28}$$

In the following we have concentrated on scenarios where only the two-body decay modes are possible. We adopt the framework of Supergravity unification as in [83] in order to reduce the number of free SUSY parameters. However, we keep ϵ_3 and v_3 as free parameters for the moment. In Fig. 29a we show the areas in the $m_{\tilde{t}_1}$-$m_{\tilde{\chi}_1^0}$ plane where the branching ratio $\tilde{t}_1 \to \tau^+ + b$ is larger than 90% for different values of ϵ_3 and v_3. We restrict to the range $|\epsilon_3|, |v_3| < 1$ GeV, and vary randomly the MSSM parameters keeping $m_{\tilde{t}_1} < m_{\tilde{\chi}_1^\pm} + m_b$. This demonstrates that one can get a dominance of the R-Parity violating decay mode even for relatively small values of the R-parity breaking parameters. The upper–left triangular region corresponds to $m_{\tilde{t}_1} < m_{\tilde{\chi}_1^0} + m_c$ and thus $BR(\tilde{t}_1 \to b\tau) = 1$. In the lower–right triangular region $m_{\tilde{t}_1} > m_{\tilde{\chi}_1^+} + m_b$ and therefore $\tilde{t}_1 \to b\,\tilde{\chi}_1^+$ is open. In the central region the top-squark has the two decay modes $\tilde{t}_1 \to b\,\tau$ and $\tilde{t}_1 \to c\,\tilde{\chi}_1^0$. The solid lines, defined by the maximum value of $|\epsilon_3|$ and $|v_3|$, are the boundary of the regions where $BR(\tilde{t}_1 \to b\tau) > 0.9$ such that points at the left of the boundary satisfy that condition.

Since BRPV models allow the decay ($\tilde{t}_1 \to \tau^+ + b$) we can interpret the top squark as a third generation leptoquark. Therefore we can use the limits obtained from leptoquark searches [36,37] to derive limits on the top-squark for this case. In Fig. 29b we show an exclusion plot in the m_0-$m_{1/2}$ plane. The nearly horizontal dashed lines are chargino mass contours and the lines forming radial patterns are the top-squark mass contours. The upper to the lower radial curves corresponds to $m_{\tilde{t}_1} = 120, 100$ and 80. The region limited by the dotted-dashed line is defined by $m_{\tilde{t}_1} < m_{\tilde{\chi}_1^+}$. The analysis rules out m_0 and $m_{1/2}$ points in the dark hashed region. In the lower hashed region no points with radiative electroweak symmetry breaking can be found. We have taken $\tan\beta = 3$, $A_0 = -650$ GeV and $\epsilon_3/\mu = -0.5$ and verified that in this region $BR(\tilde{t}_1 \to b\tau) = 1$. The Tevatron limits can not be directly applied when $A_0 > -500$ GeV, because in this case $m_{\tilde{t}_1} > m_{\tilde{\chi}_1^+} + m_b$. The regions in the m_0–$m_{1/2}$ plane where $m_{\tilde{t}_1} < m_{\tilde{\chi}^+}$ are excluded if $-650 < A_0 < -500$ GeV and $|\epsilon_3/\mu|$ is sufficiently large so that the three-body decays are negligible. Fig. 29a shows that the region where $m_{\tilde{t}_1} < m_{\tilde{\chi}_1^+} + m_b$ and $BR(\tilde{t}_1 \to \tau^+ + b) \approx 1$ is practically ruled out by experiment. For this particular choice of SUSY parameters there is only a little window still to explore at the Run II of the Tevatron. However for other choices of SUSY parameters, e.g. $A_0 = -900$ GeV the dark-hatched region fills up only about half of the allowed region where $m_{\tilde{t}_1} < m_{\tilde{\chi}_1^+} + m_b$ and would therefore be open for investigation at the next run.

The MSSM three-body channels could be competitive with the BRPV one if $|\epsilon_3/\mu|$ is very small and $m_0 \ll m_{1/2}$. In this case the condition $BR(\tilde{t}_1 \to \tau^+ + b) \approx 1$ no longer holds and our analysis is not applicable. If $|\epsilon_3/\mu| < 10^{-3}$ (which leads to tau neutrino mass in the 10^{-2}eV range in the mSUGRA model) for the same value of $\tan\beta$ we find [98] that the decay mode into $c\,\tilde{\chi}_1^0$ is competitive with the $b\tau$ channel. The $\tilde{t}_1 \to c\tilde{\chi}_1^0$ channel becomes more important for large $\tan\beta$ and $m_{\tilde{t}_1} < m_{\tilde{\chi}_1^+}$. In this case one needs $|\epsilon_3/\mu| > 10^{-2}$ in order to get a negligible $BR(\tilde{t}_1 \to c\tilde{\chi}_1^0)$.

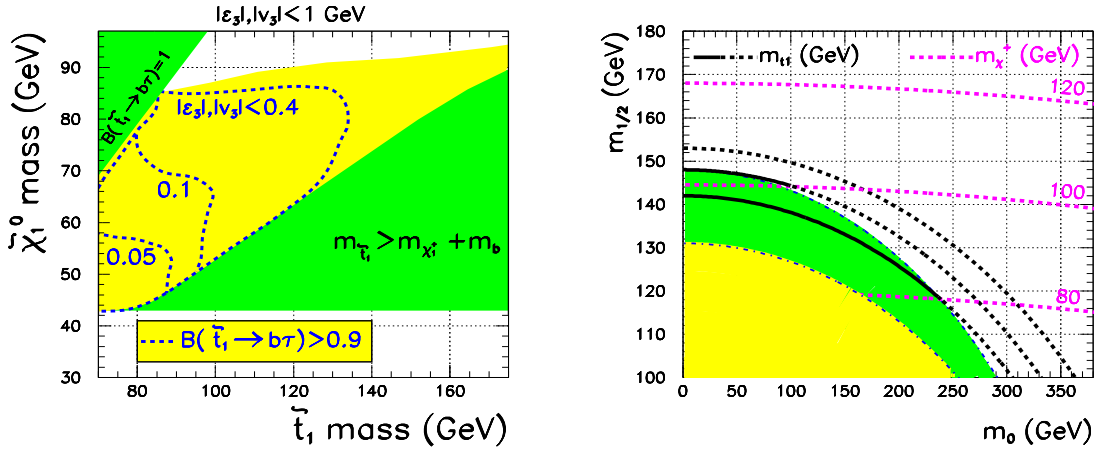

FIGURE 29. (a) Contour-lines for BR($\tilde{t}_1 \to b\tau$) > 0.9 in the $m_{\tilde{t}_1}$–$m_{\tilde{\chi}^0_1}$ plane. The gray region shows the area where only those two decay modes are open. We consider $|\epsilon_3|, |v_3| < 1$ GeV, and the MSSM parameters are varied randomly such that $m_{\tilde{t}_1} < m_{\tilde{\chi}^\pm_1} + m_b$. The lines are defined by the maximum value of $|\epsilon_3|$ and $|v_3|$ and delimit the regions where $BR(\tilde{t}_1 \to b\tau) > 0.9$. (b) Exclusion contour in the m_0–$m_{1/2}$ plane. The nearly horizontal dashed lines are chargino mass contours while the radial-like dashed lines are the top-squark mass contours. These change from solid to dashed when the top–squark becomes heavier than the lightest chargino. The radial curves correspond to $m_{\tilde{t}_1} = 120, 100$ and 80, respectively, from upper to the lower. The region limited by the dotted-dashed line has $m_{\tilde{t}_1} < m_{\tilde{\chi}^+}$. The dark hashed region is excluded by experimental data while the lower light-hashed region is disfavoured by theory. We have fixed $\tan\beta = 3$, $A_0 = -650$ GeV and $\epsilon_3/\mu = -0.5$.

D Summary

We have studied top-quark and top-squark decays in a supersymmetric model with bilinear R-parity breaking. We have found that in both cases there exist additional top and stop decay modes leading to novel phenomenological implications with respect to those of the MSSM. In the top-quark case the new decay modes are $t \to \tilde{\tau}^+_1 b$, $t \to \nu_\tau \tilde{t}_1$, and $t \to \tau^+ \tilde{b}_1$. We have shown that existing data on non-W top decay from the Tevatron are already sensitive to the BRPV parameters, adding both sbottom and stau decay channels.

In this model the top-squark has the additional channel $\tilde{t}_1 \to \tau^+ + b$. This channel will be 100% if the stop is the lightest SUSY particle, which is possible in the BRPV model. Moreover, we have demonstrated that this decay can be dominant even when the lightest neutralino below the stop and the R-parity breaking parameters $|\epsilon_3|$ and $|v_3|$ are well below a GeV, as long as the R-parity conserving chargino decay mode is kinematically closed, i.e. for $m_{\tilde{t}_1} < m_{\tilde{\chi}^+_1}$. We have studied scenarios in a SUGRA model with universality of the soft breaking terms at the unification scale and we have found that the Tevatron data on third generation lepto-quark data rule out scalar-top masses below 80-100 GeV, depending on the parameters.

Acknowledgments: This work was supported by DGICYT under grant PB95-1077 and Acción Integrada Hispano-Austriaca HU1997-0046, by the TMR network grant ERBFMRX-CT96-0090 of the European Union, by CNPq and FAPESP (Brazil), by Programa de Apoio a Núcleos de Excelência (PRONEX), by a CSIC-CNPq exchange agreement. D. A. R. was supported by Colombian COLCIENCIAS fellowship. W. P. was supported by the "Fonds zu Förderung der wissenschaftlichen Forschung" of Austria, project No. P13139-PHY. L. N. was supported by spanish CSIC fellowship.

Note Added in Proof: After this report was submitted a further slepton production process via R-parity

violation was discussed in the literature [99].

REFERENCES

1. H. Dreiner, hep-ph/9707435, published in *Perspectives on Supersymmetry*, ed. by G.L. Kane. See also P. Roy, hep-ph/9712520.
2. *Report of the Group on R-parity Violation*, R. Barbier, *et al.*, hep-ph/9810232.
3. L.J. Hall, M. Suzuki, Nucl. Phys. B231 (1984) 419.
4. B. Allanach, A. Dedes, H. Dreiner, hep-ph/9906209.
5. A nice update of the lepton number violating bounds can be found at: F. Ledroit and G. Sajot, GDR-S-008, http://qcd.th.u-psud.fr/GDR_SUSY/GDR_SUSY_PUBLIC/entete_note_publique.
6. G. Bhattacharyya, In 'Beyond the Desert', Tegernsee, Germany, June 1997, hep-ph/9709395.
7. B.A. Campbell, S. Davidson, J. Ellis, K.A. Olive, Phys. Lett. B256 (1991) 457; Astropart. Phys. 1 (1992) 77; W. Fischler, G.F. Giudice, R.G. Leigh, S. Paban, Phys. Lett. B258 (1991) 45.
8. H. Dreiner, G.G. Ross, Nucl. Phys. B410 (1993) 188, hep-ph/9207221.
9. V. Barger, G.F. Giudice and T. Han, Phys. Rev. D **40**, 2987 (1989).
10. R.M. Godbole, R.P. Roy and X. Tata, Nucl. Phys. B **401**, 67 (1993).
11. M. Hirsch, H.V. Klapdor-Kleingrothaus and S.G. Kovalenko, Phys. Rev. Lett. **75**, 17 (1995); Phys. Rev. D **53**, 1329 (1996).
12. K.S. Babu and R.N. Mohapatra, Phys. Rev. Lett. **75**, 2276 (1995).
13. J. Ellis, G. Bhattacharyya and K. Sridhar, Mod. Phys. Lett. A **10** 1583 (1995).
14. J.L. Goity and M. Sher, Phys. Lett. B **346**, 69 (1995); *erratum* Phys. Lett. B **385**, 500 (1996).
15. S.C. Bennett, C.E. Wieman, Phys. Rev. Lett. 82 (1999) 2484, hep-ex/9903022; C.S. Wood, *et al.*, Science 275 (1997) 1759.
16. J.M. Yang, hep-ph/9905486.
17. C. Caso et al, Eur. Phys. Jnl 3 (1998) 1.
18. F. Zwirner, Phys. Lett. B **132**, 103 (1983).
19. G. Bhattacharyya, D. Choudhury and K. Sridhar, Phys. Lett. B **355**, 193 (1995).
20. J. Ellis, J.S. Hagelin, D.V. Nanopoulos, K. Olive, M. Srednicki, Nucl.Phys. B 238 (1984) 453.
21. S. Dimopoulos, R. Esmailzadeh, L.J. Hall, G.D. Starkman, Phys. Rev. D41 (1990) 2099.
22. H. Dreiner, G.G. Ross, Nucl. Phys. B365 (1991) 597.
23. See the contribution by G. Landsberg in this workshop.
24. S. Dawson, Nucl. Phys. B261 (1985) 297.
25. F. Abe, *et al.*, "Search for R-parity Violating Supersymmetry using Like-Sign Dielectrons in $p\overline{p}$ Collisions at $\sqrt{s} = 1.8$ TeV," Submitted to Phys. Rev. Lett.
26. See http://www-d0.fnal.gov/public/new/analyses/rpareejjjj/welcome.html and N. Parua. *"Search for R-parity Violating Supersymmetry in $p-\overline{p}$ Collisions at $\sqrt{s} = 1.8$ TeV"*, Ph.D thesis, University of Mumbai, 1998 (unpublished).
27. J. Kalinowski, R. Ruckl, H. Spiesberger, P.M. Zerwas, Phys. Lett. B 414 (1997) 297, hep-ph/9708272.
28. A. Datta, J.M. Yang, B.L. Young, X. Zhang, Phys. Rev. D 56 (1997) 3107, hep-ph/9704257; J.M. Yang, A. Datta, M. Hosch, C.S. Li, R.J. Oakes, K. Whisnant, B.L. Young, X. Zhang, hep-ph/9802305; R.J. Oakes, K. Whisnant, J.M. Yang, B.L. Young, X. Zhang, Phys. Rev. D 57 (1998) 534, hep-ph/9707477.
29. D.P. Roy Phys Lett B283 (1992) 270.
30. V. Barger, M.S. Berger, P. Ohmann, R.J.N. Phillips, Phys. Rev. D 50 (1994) 4299, hep-ph/9405245.
31. H. Baer, C. Kao, X. Tata, Phys. Rev. D 51 (1995) 2180, hep-ph/9410283.
32. M. Guchait, D.P. Roy, Phys. Rev. D54 (1996) 3276, hep-ph/9603219.
33. C. Adloff *et al.* (H1 Collaboration), Z. Phys. C **74**, 191 (1997); J. Breitweg *et al.* (ZEUS Collaboration), Z. Phys. C **74**, 207 (1997).
34. G. Altarelli, J. Ellis, G.F. Giudice, S. Lola, M. L. Mangano, Nucl. Phys. B506 (1997) 3, hep-ph/9703276; H. Dreiner, P. Morawitz, Nucl. Phys. B 503 (1997) 55, hep-ph/9703279; J. Kalinowski, R. Ruckl, H. Spiesberger, P.M. Zerwas, Z. Phys. C74 (1997) 595, hep-ph/9703288; D. Choudhury, S. Raychaudhuri, Phys. Lett. B 401 (1997) 54, hep-ph/9702392.
35. J.L Hewett and T.G. Rizzo, Phys. Rev. **D56** 5709 (1997) and Phys. Rev. **D58** 055005 (1998) .
36. DØ Collaboration, B. Abbott *et al.*, Phys. Rev. Lett. **79**, 4321 (1997); Phys. Rev. Lett. **80**, 2051 (1998) .
37. CDF Collaboration, F. Abe *et al.*, Phys. Rev. Lett. **79**, 4327 (1997).
38. CDF and D0 Collaborations (Carla Grosso-Pilcher et al.). FERMILAB-PUB-98-312-E.
39. H. Dreiner, M. Kramer, P. Morawitz, C97-06-08.1, in *Tegernsee 1997, Beyond the desert.
40. R. Kalinowski *et al.*, Phys. Lett. **B406**, 314 (1997) and Phys. Lett. **B414**, 297 (1997) ; J.Erler, J.L. Feng and N.

Polonsky, Phys. Rev. Lett. **78**, 3063 (1997) ; B.C. Allanach *et al.*, hep-ph/9708495; S.Bar-Shalom, G.Eilam and A. Soni, hep-ph/9804339 and hep-ph/9802251; J.L. Feng, J.F. Gunion and T. Han, hep-ph/9711414.
41. T.G. Rizzo, hep-ph/9609248, published in the *New Directions for High High Energy Physics, Proceedings of the 1996 DPF/DPB Summer Study on High Energy Physics*, eds. D.G Cassel, L.T. Gennari and R.H. Siemann, Snowmass, CO 1996.
42. F. Abe *et al.*, CDF Collaboration, Phys. Rev. Lett. **77**, 5336 (1996) , Erratum, *ibid.*, **78**, 4307 (1997); R. Harris, in *Proceedings of the 10th Topical Workshop on Proton-Antiproton Collider Physics*, Batavia, IL 1995, ed. R. Raja and J. Yoh; S. Abachi *et al.*, D0 Collaboration, in the *Proceedings of the 28th International Conference on High Energy Physics*, Warsaw, Poland, July 1996, FERMILAB-CONF-96-168-E and hep-ph/9807014.
43. *Future Electroweak Physics at the Fermilab Tevatron*, eds D. Amidei and R. Brock, Fermilab-Pub-96/082.
44. J.L. Hewett and T.G. Rizzo, Phys. Rep. **183**, 193 (1989) .
45. F. Abe *et al.*, CDF Collaboration, Phys. Rev. Lett. **77**, 2616 (1996) .
46. F. Abe *et al.*, CDF Collaboration, Phys. Rev. Lett. **74**, 850 (1995) and hep-ex/9809001.
47. J. Butterworth, H. Dreiner, *Nucl. Phys.* **B397** (1993) 3.
48. E. Perez, Y. Sirois, H. Dreiner, Presented at Workshop on Future Physics at HERA, hep-ph/9703444.
49. CDF Collaboration (Jane Nachtman et al.), FERMILAB-CONF-99-023-E, hep-ex/9902010.
50. S. Moretti, K. Odagiri, M.H. Seymour and B.R. Webber 'Implementation of supersymmetric processes in the HERWIG event generator', *preprint* Cavendish-HEP-98/06, currently in preparation.
51. G. Marchesini, B.R. Webber, G. Abbiendi, I.G. Knowles, M.H. Seymour and L. Stanco, *Comp. Phys. Comm.* **67** (1992) 465.
52. G. Corcella, I.G. Knowles, G. Marchesini, S. Moretti, K. Odagiri, M.H. Seymour and B.R. Webber, 'HERWIG version 6.1, including supersymmetric processes in hadronic collisions', *preprint* Cavendish-HEP-98/04, currently in preparation.
53. F.E. Paige, S.D. Protopescu, H. Baer and X. Tata, 'Isajet 7.40', *preprint* hep-ph/9810440.
54. R. Bonciani, S. Catani, M.L. Mangano, P. Nason, *Nucl. Phys.* **B529** (1998) 424.
55. E.A. Baltz and P. Gondolo, *Phys. Rev.* **D57** (1998) 2969.
56. H. Dreiner, P. Morawitz, *Nucl. Phys.* **B428** (1994) 31, hep-ph/9405253.
57. M. Hirsch, H.V. Klapdor-Kleingrothaus, S.G. Kovalenko, *Phys. Rev. Lett.* **75** (1995) 17; *Phys. Rev.* **D53** (1996) 1329, hep-ph/9502385.
58. J. Ellis and S. Rudaz, Phys. Lett. B 128 (1983) 248.
59. E. L. Berger, B. W. Harris, and Z. Sullivan, hep-ph/9903549, Argonne National Laboratory Report ANL-HEP-PR-99-05, March 1999.
60. S. Weinberg, Phys. Rev. D **26**, 287 (1982); N. Sakai and T. Yanagida, Nucl. Phys. **B197**, 533 (1982).
61. CTEQ Collaboration, H. Lai *et al.*, Phys. Rev. D **55**, 1280 (1997).
62. A. Chamseddine, R. Arnowitt, and P. Nath, Phys. Rev. Lett. **49**, 970 (1982); R. Barbieri, S. Ferrara, and C. A. Savoy, Phys. Lett. B**119**, 343 (1982); L. J. Hall, J. Lykken, and S. Weinberg, Phys. Rev. D **27**, 2359 (1983).
63. T. Stelzer and W. F. Long, Comput. Phys. Commun. **81**, 357 (1994).
64. F. Abe *et al.* (CDF Collaboration), Nucl. Instrum. Methods A**271**, 387 (1988), and references therein; D. Amidei *et al.*, Nucl. Instrum. Methods A**350**, 73 (1994); F. Abe *et al.* (CDF Collaboration), Phys. Rev. **D50**, 2966 (1994).
65. The CDF II Detector Technical Design Report, Fermilab-Pub-96/390-E, 1996.
66. D. Choudhury and S. Raychaudhuri, Phys. Lett. **B401**, 54 (1997).
67. D. Choudhury and S. Raychaudhuri, Phys. Rev. **D56** 1778 (1997).
68. Bounds on λ_{121} are derived from tests of charged current universality: V. Barger, G. Guidice, and T. Han, Phys. Rev. **D40** 2987 (1989), Particle Data Group, Phys. Rev. **D54** 1 (1996).
69. R. Brun and F. Carminati, CERN Program Library Writeup W5013, 1993 (unpublished). We used GEANT version 3.15.
70. T. Hu and P. Quintas, DØ Note # 2956 (unpublished).
71. D. Wirjawan. *"A search for Wino-Zino Associated Production via Trilepton final states"*. Ph.D. thesis, Texas A& M University, 1998 (unpublished).
72. A. Brignole, L.E. Ibanez, and C. Munoz, Nucl. Phys. **B**, 4 (2)2 125 1994 , Erratum, *ibid.*, **B436** 747 (1995); CERN-TH/97-143 [hep-ph/9707209].
73. G. Giudice, M. Luty, H. Murayama and R. Rattazzi, hep-ph/9810442.
74. L. Randall and R. Sundrum, hep-th/9810155.
75. G. Anderson, C.H. Chen, J.F. Gunion, J. Lykken, T. Moroi and Y. Yamada, hep-ph/9609457, published in *New Directions for High Energy Physics*, Proceedings of the Snowmass96 Summer Study, June 25 – July 12, 1996, Snowmass CO, eds. D.G. Cassel, L.T. Gennari, and R.H. Siemann, p. 669.
76. C.H. Chen, M. Drees, and J.F. Gunion, Phys. Rev. Lett. **7**, 6 (2)002 1996 .
77. C.H. Chen, M. Drees, and J.F. Gunion, Phys. Rev. **D** 5 (5) 330 1997 .

78. J.F. Gunion and S. Mrenna, these proceedings.
79. D. Chang and W.-Y. Keung, Phys. Lett. **B**, 3 (8)9 294 1996 .
80. R. Barbieri and A. Masiero, Nucl. Phys. **B**, 2 (6)7 679 1986 .
81. We thank R. Demina and H. Fritsch for communicating details of CDF efficiencies to us.
82. H. Baer, K. Cheung, J.F. Gunion, work in progress.
83. M. A. Díaz, J. C. Romão, and J. W. F. Valle, *Nucl. Phys.* **B524** 23 (1998).
84. M. A. Díaz, hep-ph/9711435, hep-ph/9712213; J. C. Romão, hep-ph/9712362; J. W. F. Valle, talk at PASCOS 98, hep-ph/9808292.
85. F. de Campos, M. A. García-Jareño, A. S. Joshipura, J. Rosiek, and J. W. F. Valle, *Nucl. Phys.* **B451**, 3 (1995); A. Akeroyd, M. A. Díaz, J. Ferrandis, M. A. García-Jareño, J. W. F. Valle, *Nucl. Phys.* **B529**, 3 (1998).
86. A. S. Joshipura and M. Nowakowski, *Phys. Rev. D* **51**, 2421 (1995); T. Banks, Y. Grossman, E. Nardi, and Y. Nir, *Phys. Rev. D***52**, 5319 (1995); F. Vissani and A. Yu. Smirnov, *Nucl. Phys.* **B460**, 37 (1996); R. Hempfling, *Nucl. Phys.* **B478**, 3 (1996); F. M. Borzumati, Y. Grossman, E. Nardi, Y. Nir, *Phys. Lett.* **B384**, 123 (1996); H. P. Nilles and N. Polonsky, *Nucl. Phys.* **B484**, 33 (1997); B. de Carlos, P. L. White, *Phys. Rev. D***55**, 4222 (1997); E. Nardi, *Phys. Rev. D***55**, 5772 (1997); S. Roy and B. Mukhopadhyaya, *Phys. Rev. D***55**, 7020 (1997); A. Faesiter, S. Kovalenko, F. Simkovic, *Phys. Rev. D***58**, 055004 (1998); M. Carena, S. Pokorski, and C. E. M. Wagner, *Phys.Lett.* **B430**, 281 (1998); M. E. Gómez and K. Tamvakis, *Phys.Rev. D* **58**, 057701 (1998).
87. A. Masiero and J. W. F. Valle, *Phys. Lett.* **B251**, 273 (1990); J. C. Romão, A. Ioannissyan, and J. W. F. Valle, *Phys. Rev. D***55**, 427 (1997).
88. M. A. Díaz, J. Ferrandis, J. C. Romão, and J. W. F. Valle, hep-ph/9801391.
89. For reviews see J. W. F. Valle, hep-ph/9712277 and hep-ph/9603307.
90. V. Berezinskii, A. S. Joshipura, J. W. F. Valle. *Phys. Rev. D***57**, 147-151 (1998).
91. H. Dreiner and R. J. N. Phillips, *Nucl. Phys.* **B367**, 591 (1991); V. Barger, M. S. Berger, R. J. N. Phillips, T. Wöhrmann. *Phys. Rev. D***53** ,6407 (1996).
92. CDF Coll., F. Abe et al.,*Phys. Rev. Lett.* **74**, 2626 (1995); D0 Coll., S. Abachi et al.,*Phys. Rev. Lett.* **74**, 2422 (1995); *Phys. Rev. Lett.* **74**, 2632 (1995); *Phys. Rev. D***52**, 4877 (1995).
93. S. Mrenna and C.-P. Yuan, *Phys. Lett.* **B367** 188 (1996); M. Hosch et al., *Phys. Rev. D***58**:034002 (1998); G. V. Velev (for the CDF Coll.) FERMILAB-Conf-98/192-E.
94. R. Rebecchi, talk given at ICHEP98, Vancouver, Canada, July 23-29, 1998.
95. T. LeCompte, Rare Decays Working Group Summary, workshop on top–quark physics at Run II, Fermi National Accelerator Laboratory, October 16 - 18, 1998
96. K. Hikasa, M. Kobayashi, Phys. Rev. D 36 (1987) 724; A. Bartl et al., *Z. Phys.* **C73**, 469, (1997); W. Porod and T. Wöhrmann, *Phys. Rev. D* **55**, 2907 (1997); W. Porod, hep-ph/9812230, to appear in *Phys. Rev. D.*
97. A. Bartl et al., *Phys. Lett.* **B384**, 151 (1996).
98. M. A. Díaz, D. A. Restrepo, J. W. F. Valle, in preparation.
99. F. Borzumati, J.-L. Kneur, N. Polonsky, hep-ph/9905443.